

Turbulence and structures in dispersive MHD

T. Passot, D. Laveder, G. Sanchez-Arriaga, P.L. Sulem,
D. Borgogno, L. Marradi

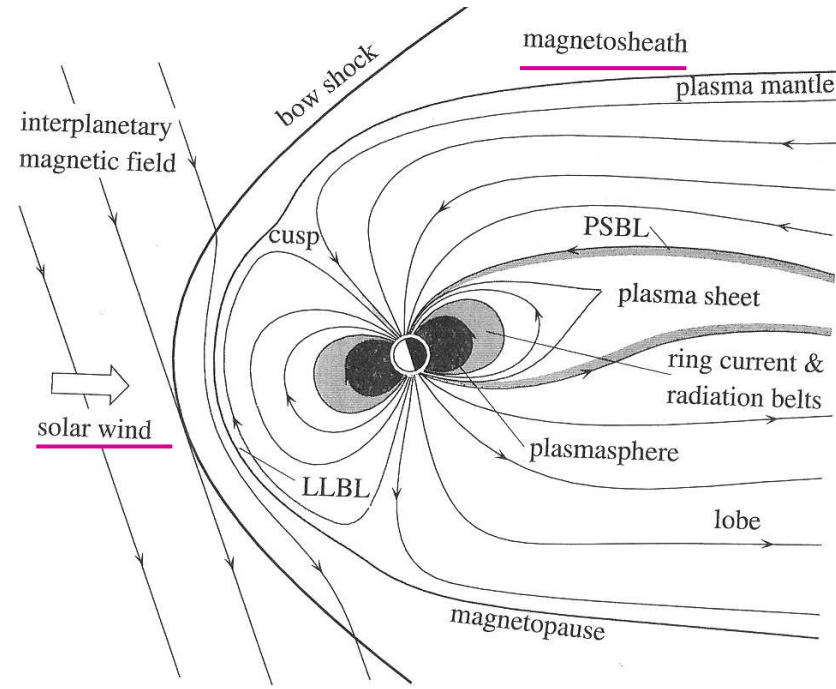
Observatoire de la Côte d'Azur, Nice, France

OUTLINE

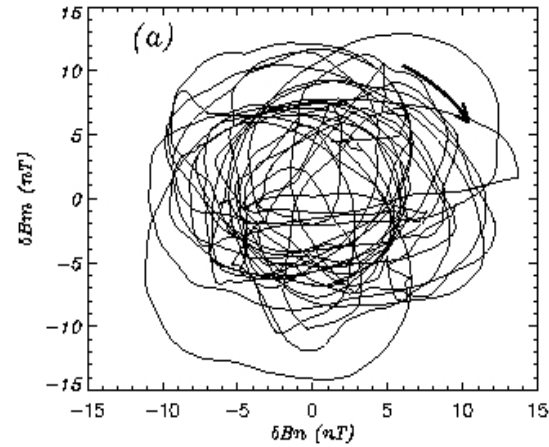
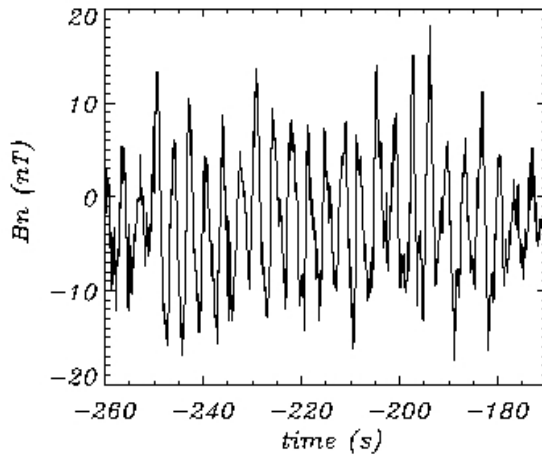
- Introduction : evidence of **dispersive Alfvén waves** in the solar wind and the terrestrial magnetosheath and of the signature of **turbulence and coherent structures**
- **Break of the spectrum at the ion gyroscale**: tentative explanations
- The simple but nevertheless complex case of the forced 1D DNLS equation
- The Landau fluid model as a tool for investigating dispersive turbulence
- Preliminary 1D Landau fluid simulations
- 2D Hall-MHD simulations

Evidence of DAWs

Quasi-monochromatic dispersive Alfvén waves are commonly observed in the solar wind and in the magnetosheath

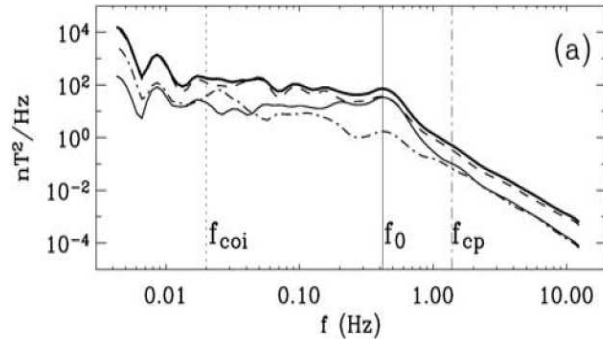


Observation by CLUSTER satellites downstream the quasi-perpendicular bow shock (Alexandrova et al., J. Geophys. Res., (2004, 2006))

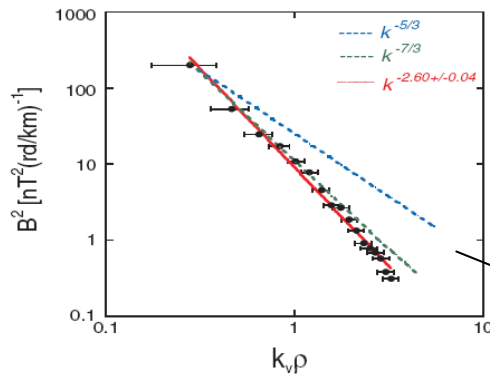


Presence of almost monochromatic left-hand circularly polarized Alfvén waves

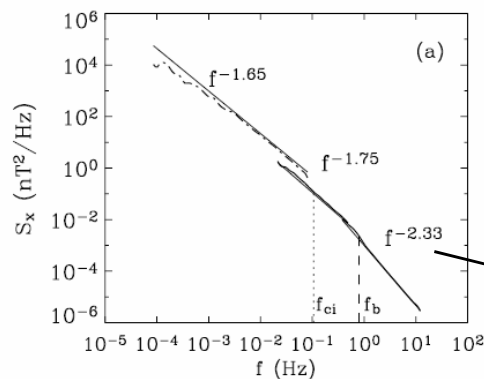
Evidence of turbulence



Magnetic energy spectrum in the magnetosheath downstream of the bow shock (Alexandrova et al., JGR, 2006).



Magnetic energy spectrum in the magnetosheath close to the magnetopause (Sahraoui et al., PRL 2006)



Solar wind turbulent spectrum (Alexandrova et al., 2007)

Space plasmas such as the solar wind or the magnetosheath are **turbulent magnetized plasmas** with essentially **no collisions**.

Observed cascade extends beyond the ion Larmor radius: **kinetic effects** play a significant role.

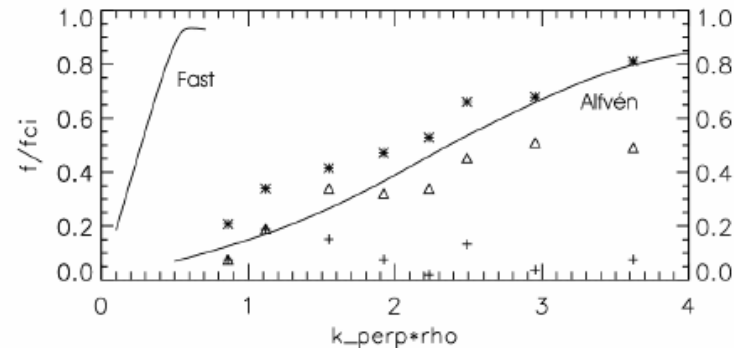
Here identified as mirror modes using k-filtering technique: modes with essentially zero frequency in the plasma frame

Range of observed frequency power law indices between -2 and -4.5 (Leamon et al. 1998)
RH polarized outward propagating waves (Goldstein et al. JGR 94)

The Alfvén wave cascade develops preferentially **perpendicularly to the ambient magnetic field**.

Assuming frequencies remain relatively small in comparison with the ion gyrofrequency, the dynamics should be dominated by **Kinetic Alfvén waves** (and slow modes, but these ones are highly dissipative).

KAWs have been clearly identified using k-filtering technique in the cusp region (Sahraoui et al. AIP, 2007).



Evidence of KAWs

Another medium where KAWs play a fundamental role is the **solar corona**, where they are believed to mediate the conversion of large-scale modes into heat.

The nature of the fluctuations associated with the power spectrum at frequencies larger than the ion-gyrofrequency in the satellite frame is however not yet established in all situations.

Another issue:

Formation and evolution of **small-scale coherent structures** (filaments, shocklets, magnetosonic solitons, magnetic holes) observed in various spatial environments :

Typical length scale of the structures:
a few ion Larmor radii.

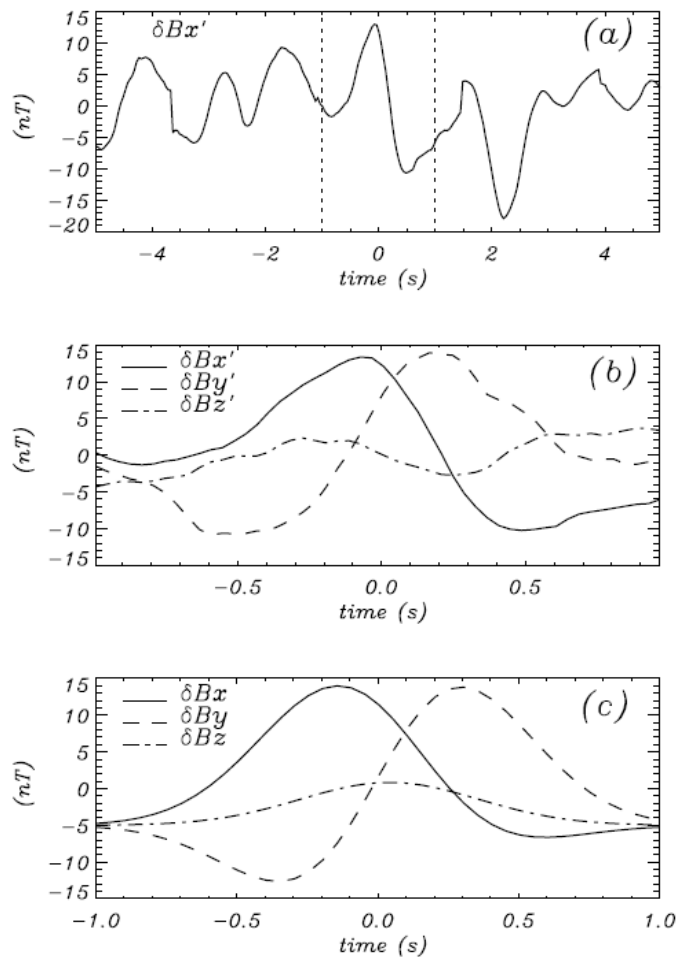


Figure 8. Magnetic field fluctuations, taking $\tau \simeq -420$ s (1755:16 UT) as the origin of time. (a) Fluctuations $\delta B_{x'}$ during 10 s around τ . (b) Fluctuations of the magnetic field components ($\delta B_{x'}$, $\delta B_{y'}$, $\delta B_{z'}$) for the 2-s period around τ . (c) The z -aligned current tube simulation (δB_x , δB_y , δB_z).

Signature of magnetic filaments (Alexandrova et al. JGR 2004)

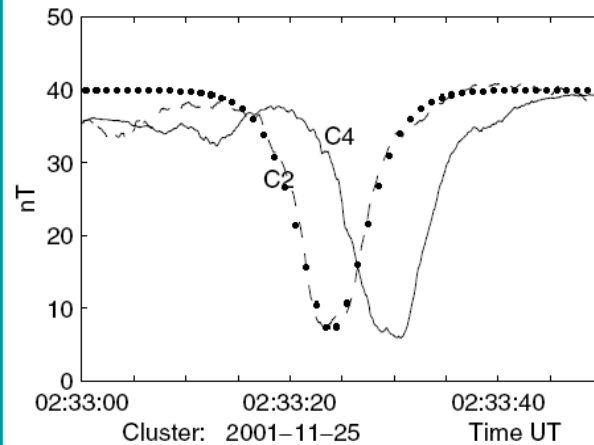


FIG. 1. A large scale soliton observed by Cluster spacecraft C2 (dashed) and C4 (solid) in the total magnetic field. Marked curve shows fit of $b_0 \text{sech}^2[(t - t_0)/\delta t]$ with $b_0 = -33$ nT and $\delta t = 4.4$ s. The soliton moves with velocity $u_0 \approx 250$ km/s and has a width of 2000 km. The position of Cluster satellites was $(-4, 17, 5) R_E$ GSE.

Slow magnetosonic solitons (Stasiewicz et al. PRL 2003)

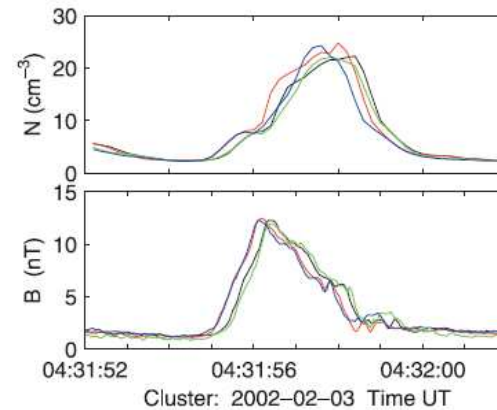
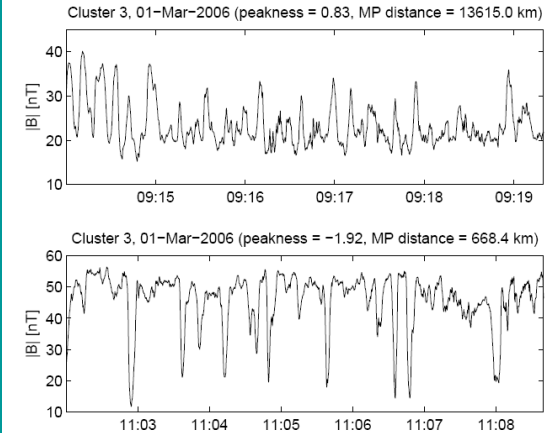


Figure 2. Pulse-like enhancements of the plasma density and magnetic field measured on four Cluster spacecraft: C1–C4, which are color coded in sequence: black, red, green, blue. The measurements represent signatures of fast magnetosonic shocklets moving with supersonic speed in a high- β plasma.



Mirror structures in the terrestrial magnetosheath (Soucek et al. JGR 2008)

fast magnetosonic shocklets (Stasiewicz et al. GRL 2003)

Question: How does **turbulence** develop at **dispersive scales**?

- Is the transfer suppressed in the parallel direction?
- Are solitonic-type structures generically formed or does weak (or strong) turbulence prevail?
- What kind of structures are formed in the transverse direction?
- What is the origin of the spectral break at the ion Larmor radius scale.

Tentative models for the « dissipation range »: I.

Whistler wave cascade in the parallel direction or magnetosonic wave cascade (and also AW) in the transverse directions are proposed as long as $\beta < 2.5$, using a diffusion equation in wavenumber space with the linear time as the energy transfer time. It leads to a k^{-3} spectrum

$$\left(\frac{\partial E(k)}{\partial t} \right)_{\text{nonlinear}} = \frac{\partial}{\partial k} \left[\frac{\gamma k^4}{4\pi\tau_S(k)} \frac{\partial [k^{-2}E(k)]}{\partial k} \right]$$

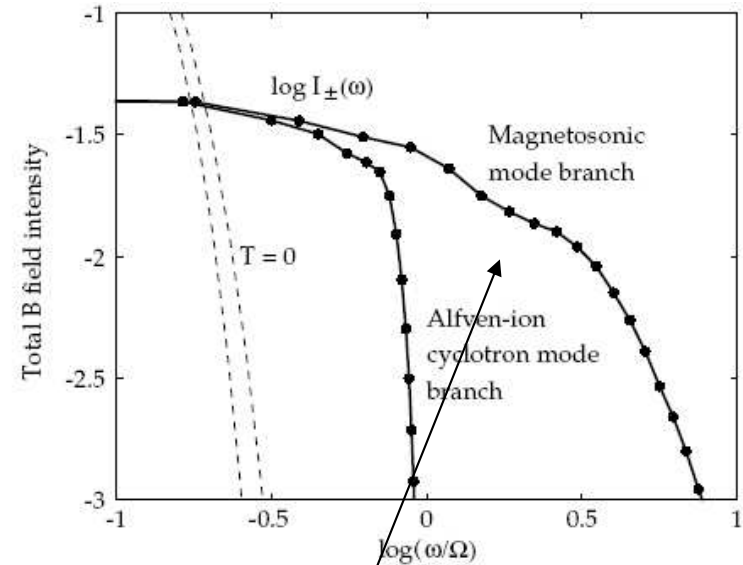
(Leith (1967), Zhou & Matthaeus, JGR 95, 14881 (1990))
(Stawicki, Gary & Li, JGR **106**, 8273 (2001)).

2D PIC simulation of whistler turbulence shows preferential cascade towards perpendicular wavenumbers with steep power laws, and no cascade in 1D
(Gary et al. GRL 35, L02104 (2008)).

BUT

Alfvén wave parallel cascade via three-wave decay: transfer from large-scale AW to small-scale ion-cyclotron and magnetosonic whistler wave mediated by ion-sound turbulence (Yoon, PPCF 50 085007 (2008)).

Weak turbulence of KAW via three-wave decay: inverse cascade if $k_{\perp}\rho_i < 1$, forward cascade otherwise (with a steeper power law). (Voitenko, JPP 60, 515 (1998)).



Note the knee in the spectrum

Tentative models for the « dissipation range »: II.

Weak turbulence for incompressible Hall MHD:

For $kd_i \gg 1$ transfer essentially perpendicular to B_0 : $k_{\perp}^{-5/2}$

For $kd_i \ll 1$ transfer exclusively perpendicular to B_0 : k_{\perp}^{-2}

(Galtier, JPP **72**, 721 (2006))

2D DNS of compressible HMHD : decaying turbulence shows steepening of the spectrum near the ion-cyclotron scale when the cross-helicity is high

(Gosh et al. JGR **101**, 2493 (1996)).

Strong incompressible HMHD simulations of shell model (without mean field): the $k^{-5/3}$ AW cascade steepens to a $k^{-7/3}$ EMHD spectrum when magnetic energy dominates and to a $k^{-11/3}$ spectrum when kinetic energy dominates

(Galtier & Buchlin, ApJ **656**, 560 (2007)).

Important role of nonlinearity in the Hall term.

Tentative models for the « dissipation range »: III.

In the MHD range, the AW cascade is essentially transverse to the ambient field. At the **ion Larmor radius**, the cascade continues with KAWs ($k_{\perp}^{-7/3}$), the turbulent fluctuations remaining below the ion cyclotron frequency due to the strong anisotropy. Gyrokinetic is thus an appropriate tool for the description of this regime.

The range of exponents for power laws could be attributed to:

- a. collisionless damping, the true behavior being an exponential fall off, the observed power law being an artifact of instrumental sensitivity?
- b. a competition with a dual cascade of entropy modes.

(Howes et al. JGR **113**, A05103 (2008), AIP, CP932 (2007), ApJ **651**, 590 (2006), Apj sup. submitted).

Observational constraints:

Recent analysis of the spectrum break point in the solar wind shows its location is not only determined by a scale of the turbulence fluctuations, but by a combination of their scale and the amplitude at that scale. It is essentially a nonlinear process.

No theory seems to be able to explain all observations.
The correlation with ion inertial length is better than with the ion gyroscale.

(Markowskii et al. ApJ **675**, 1576 (2008)).

Issues:

It is mentioned that dispersion increases the energy transfer rate, leading to steeper power laws. However it is also known that waves inhibit transfers, leading to shallower spectra (IK spectrum).

⇒ What is the true role of waves and dispersion on nonlinear transfer due to classical steepening phenomena?

Is the important scale the ion gyroradius or the ion inertial length?

Does the cascade proceed anisotropically all the way to the electron scale?

Program: Study these problems with 3D simulations of a Landau fluid model

As a first step it is convenient to study a simpler example containing one kind of waves propagating in one direction: **DNLS**

Turbulence in DNLS

Parallel propagating Alfvén waves can develop solitonic structures, as seen in the context of DNLS, a large scale 1D reduction:

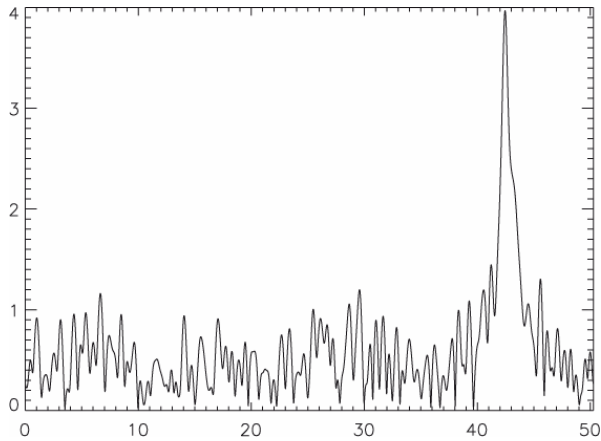
$$\partial_{\tau} b + \frac{i}{2R_i} \partial_{\xi\xi} b + \frac{1}{4(1-\beta)} \partial_{\xi} (|b|^2 b) = 0$$

What happens in the presence of external forcing?

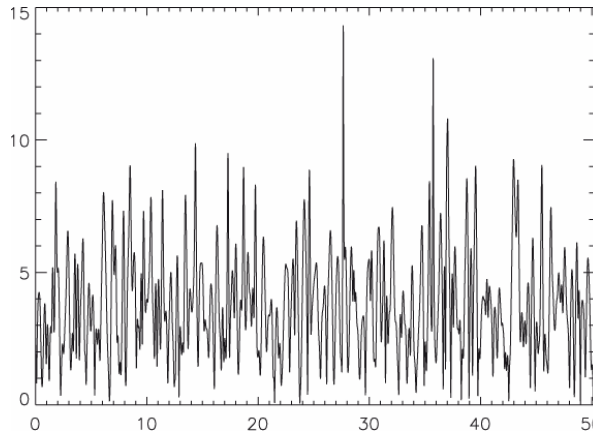
Initial condition : soliton
Harmonic forcing at $k=50$.
Very small dissipation
Energy increases and then saturates

→ Abrupt transition

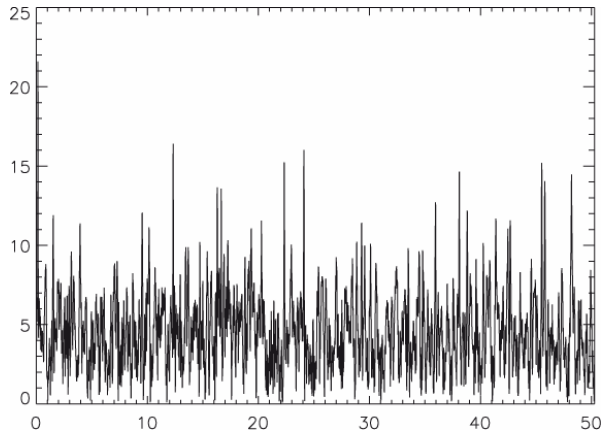
→ Second transition



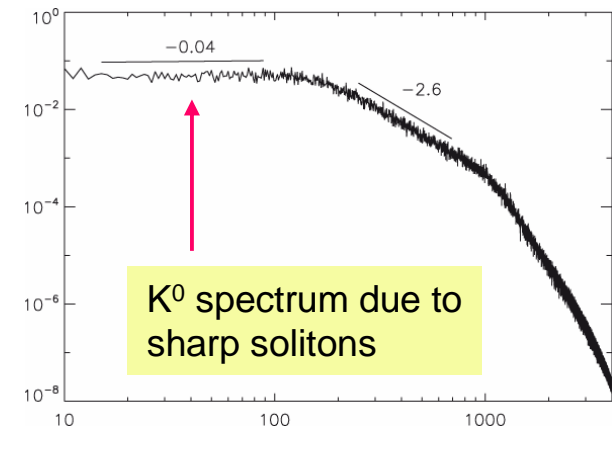
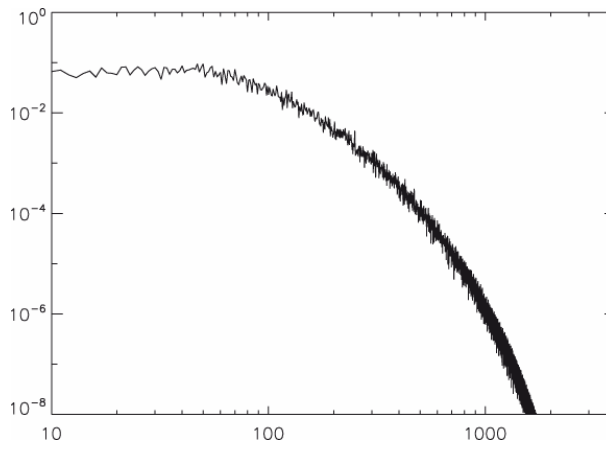
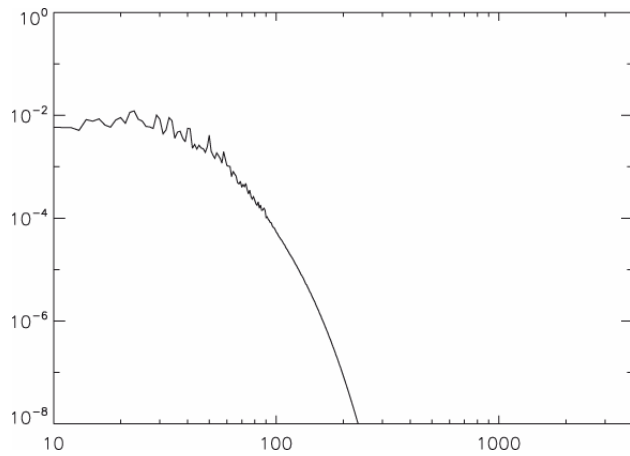
T=100



T=190

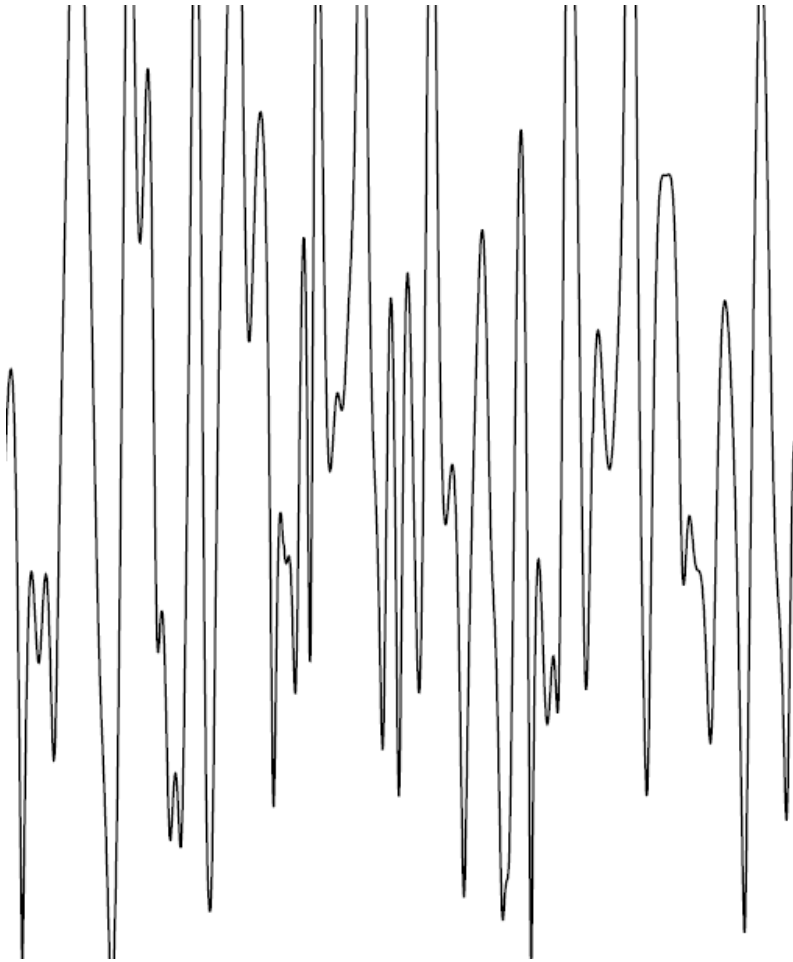


T=275

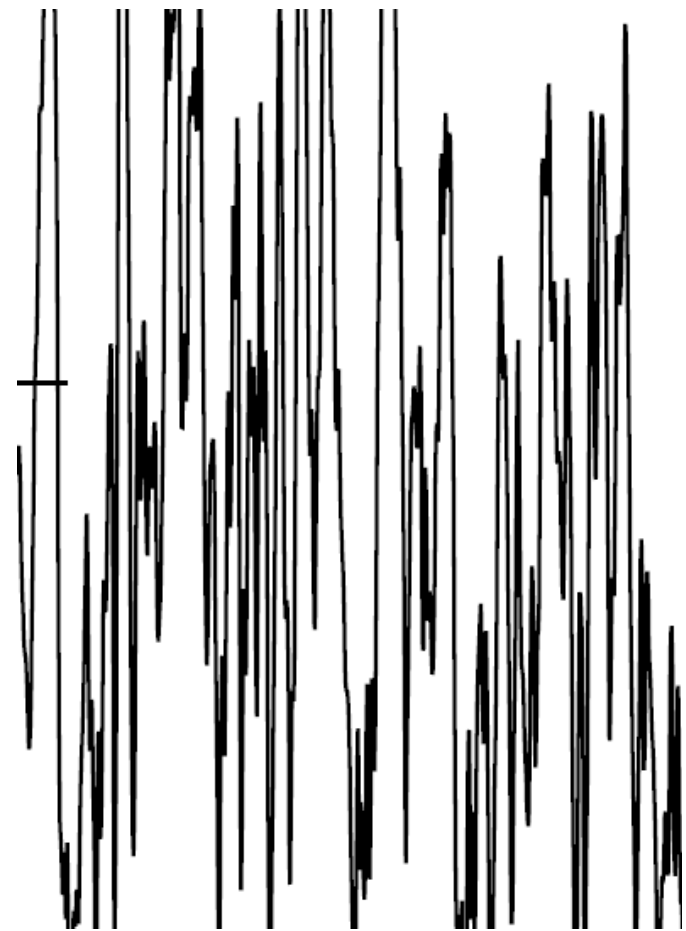


Problem initially investigated by Buti and Nocera, Solar Wind 9, AIP (1999).

Enlargement



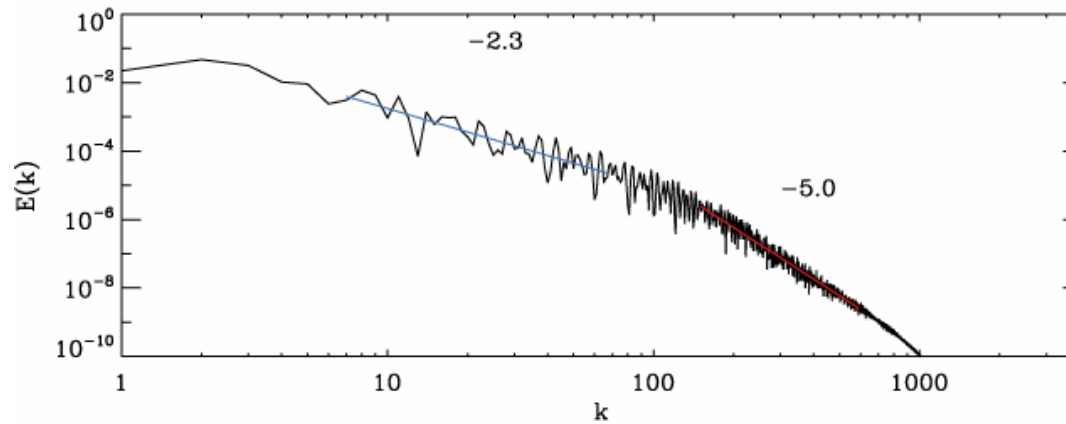
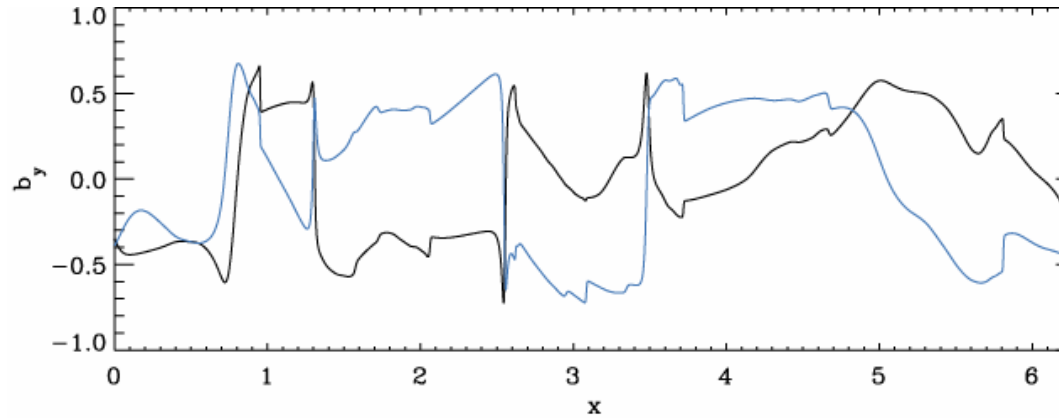
Signature of peaks: flat spectrum



Signature of superimposed oscillations: steeper spectrum at smaller scales.

Generation of turbulence with white noise in time random forcing.

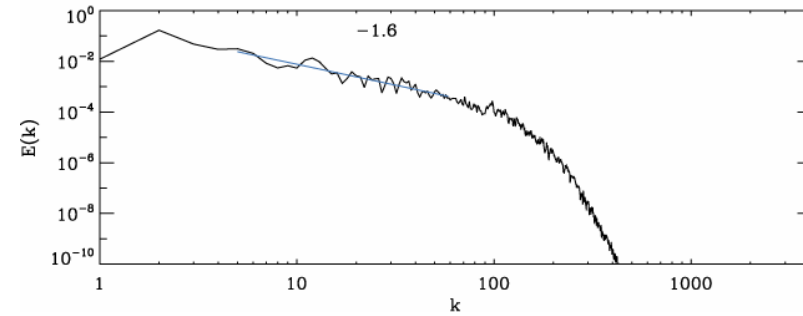
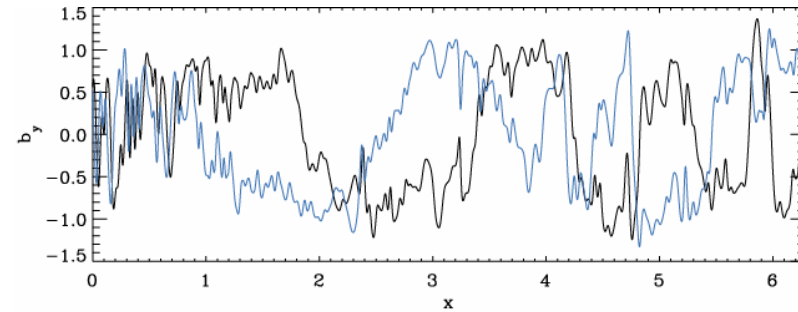
I. Case without dispersion: Cohen-Kulsrud equation



Zero initial condition
White noise forcing at $k=4$.
Newtonian viscosity
Energy increases and then saturates

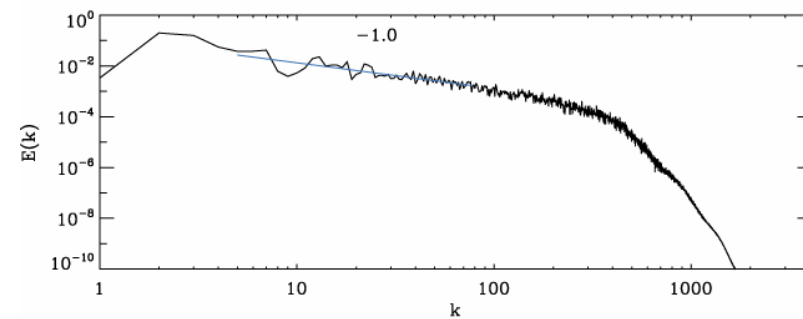
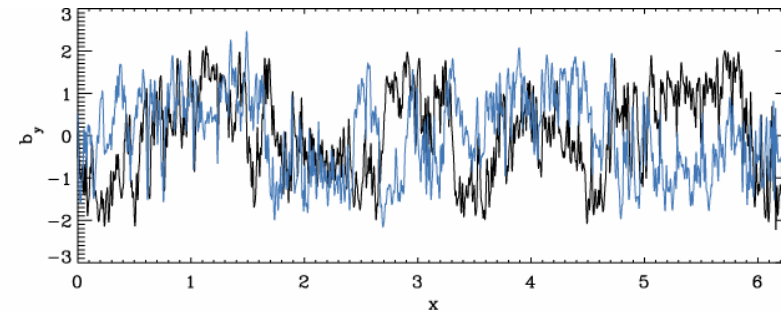
II. With small dispersion

With moderate dissipation



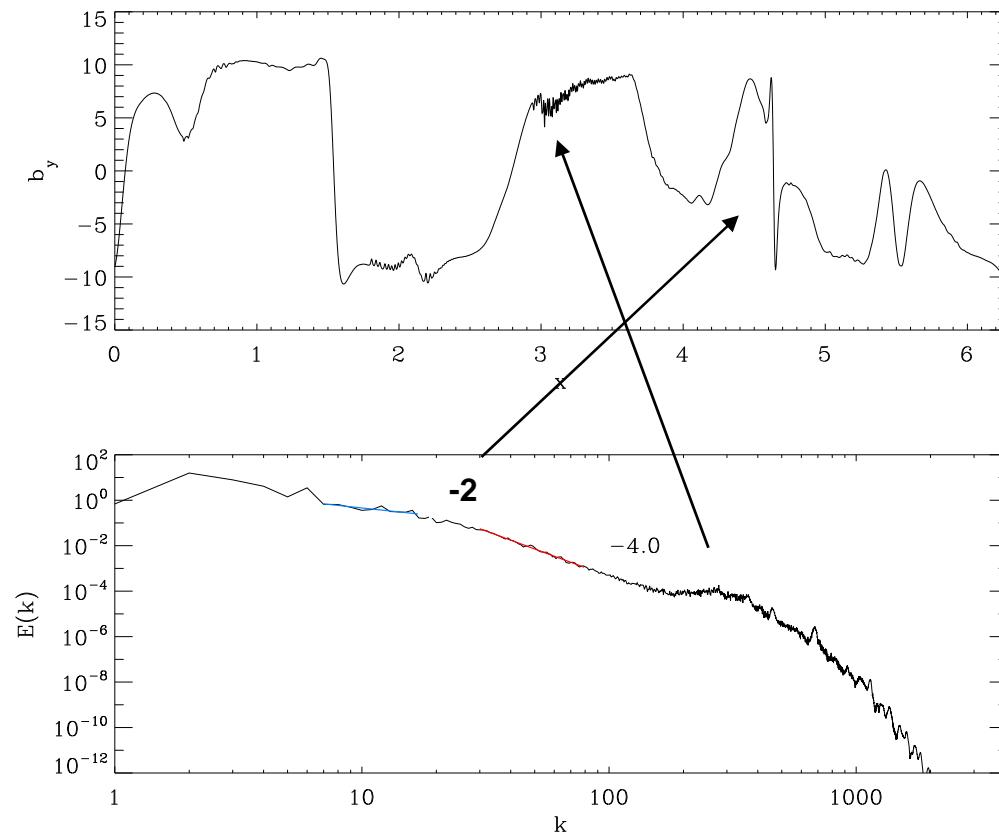
Zero initial condition
White noise forcing at $k=4$
Domain size: $400 \pi d_i$

With small dissipation



II. With larger dispersion

Dissipation: k^2 diffusivity

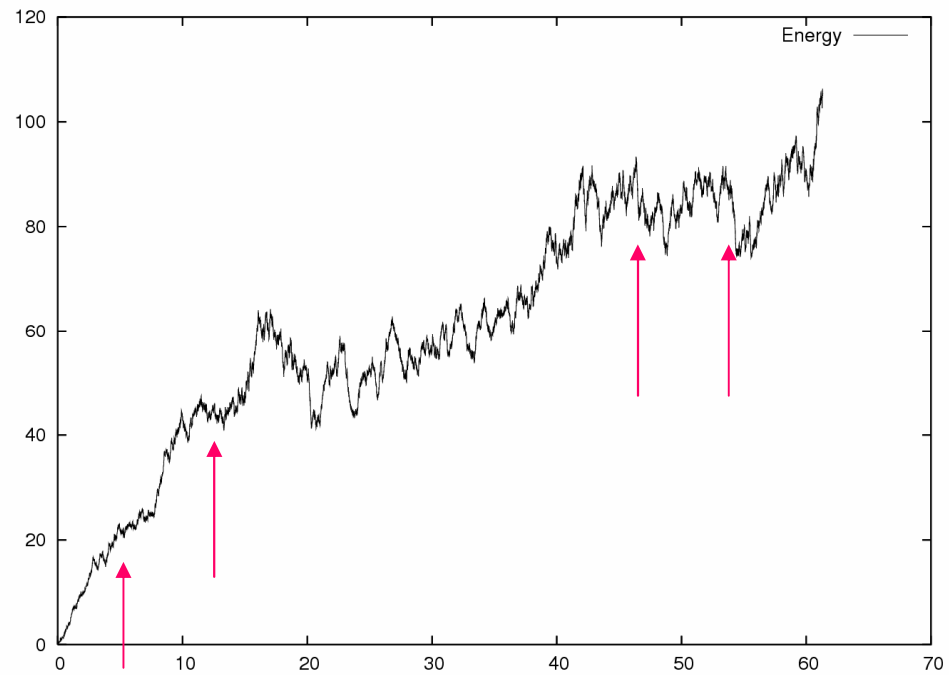


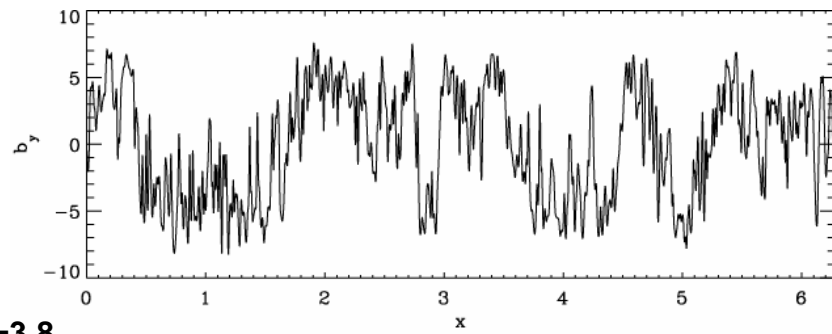
Zero initial condition
White noise forcing at $k=4$
Domain size: $16\pi d_i$

No small-scale turbulence
Dissipation dominant over
dispersion

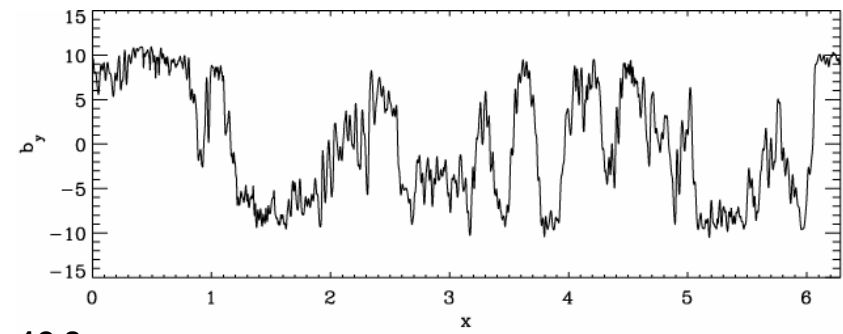
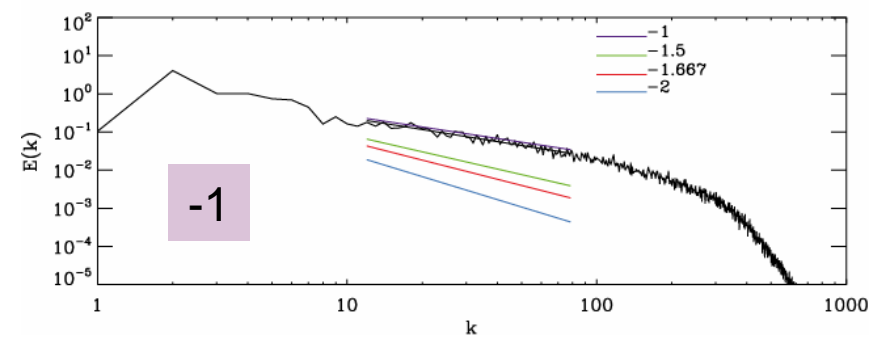
Dissipation: k^8 hyperdiffusivity

Typical evolution of energy
vs time: **no saturation!**

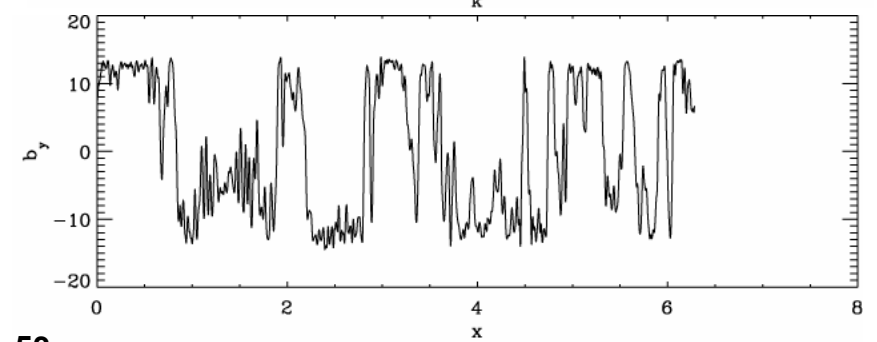
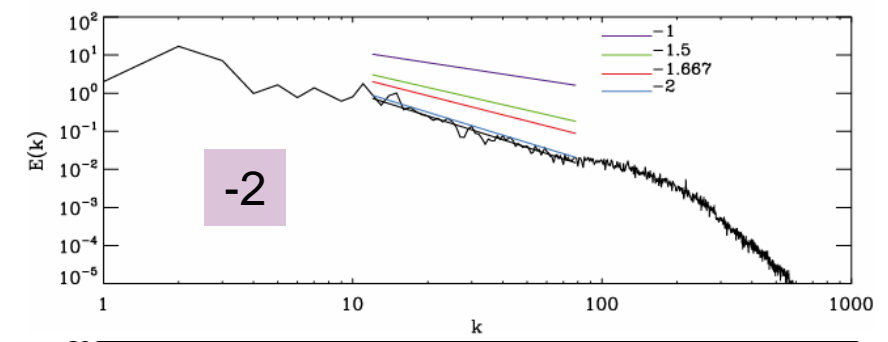




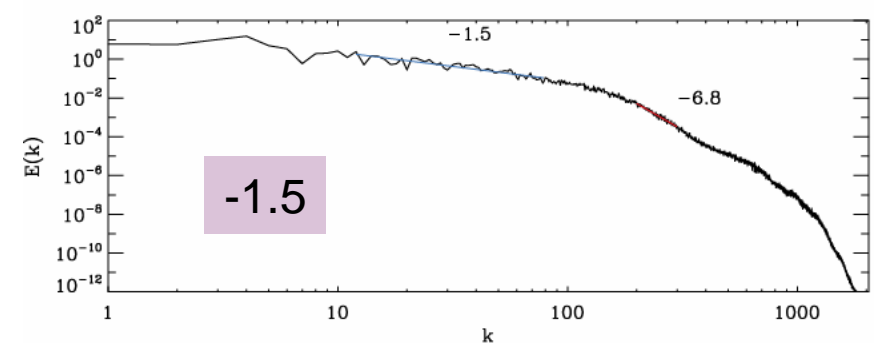
t=3,8



t=12,8



t=53



In this case dissipation is subdominant with respect to dispersion. As a result, dispersion decorrelates phases and thus structures such as shocks. Dissipation becomes intermittent in time and is dominated by « soliton collapse events ».

Measure of **nonlinear transfer** shows that it is well-defined for the Cohen-Kulsrud equation (DNLS without dispersion), while for DNLS it is dominated at smaller scales by extremely **intermittent events both in wavenumber space and in time, both positive and negative**. A more precise estimation using long-time averaging is underway in the weakly turbulent regime.

The break in the spectrum shifts to smaller scales when decreasing dissipation.

Kinetic-DNLS equation

$$\frac{\partial b}{\partial \bar{t}} + \frac{V_A}{4} \alpha \frac{\partial}{\partial \bar{\xi}} [(|b|^2 - \langle |b|^2 \rangle - \sigma \mathcal{H} \{ |b|^2 \}) b] + \frac{i V_A^2}{2 \Omega_i} \delta \frac{\partial^2 b}{\partial \bar{\xi}^2} = 0$$

where

Frame moving at velocity

$$\mathcal{H} \{ V(x) \} = \frac{1}{\pi} P \int_{-\infty}^{+\infty} \frac{V(x')}{x' - x} dx'$$

$$\bar{\xi} = x - \lambda_0 \bar{t}$$

$$\text{where } \lambda_0^2 = V_A^2 + p_{\perp} / \rho - p_{\parallel} / \rho, \quad V_A = B_0 / \sqrt{4\pi\rho}$$

$$\delta = 1 + \frac{1}{4}\beta \quad \alpha(1 - i\sigma) = 1 - \left[\frac{W^2 + 2W - 3}{4(W + 1)} \right] \beta \quad W(\beta) = \frac{1}{\sqrt{2\pi}} \lim_{\epsilon \rightarrow 0} \int_{-\infty}^{+\infty} \frac{\varsigma e^{-\frac{1}{2}\varsigma^2}}{\varsigma - \frac{2}{\sqrt{\beta}} - i\epsilon} d\varsigma(4)$$

In the limits $\beta \gg 1$ and $\beta \ll 1$ one finds

$$\beta \ll 1 \quad \alpha \simeq 1 + \frac{3}{4}\beta \quad \sigma \simeq \frac{5}{4} \sqrt{2\pi\beta} e^{-\frac{2}{\beta}}$$

$$\beta \gg 1 \quad \alpha \simeq 3 - \frac{\pi}{4} \quad \sigma \simeq \frac{1}{2} \frac{\sqrt{2\pi\beta}}{3 - \frac{\pi}{4}}$$

$$\frac{\partial b}{\partial t} + \frac{\alpha}{4} \frac{\partial}{\partial \xi} [(|b|^2 - \langle |b|^2 \rangle - \sigma \mathcal{H} \{ |b|^2 \}) b] + \frac{i \delta}{2} \frac{\partial^2 b}{\partial \xi^2} = F(x, t)$$

Nondimensional form:

The Fourier transform of the function $F(x, t)$ is given by:

$$\tilde{F}(k, t) = A_0 (a_1 + ia_2) \sqrt{\frac{h(k)}{\Delta T}} \quad h(k) = k^p e^{-\frac{k^2}{2\sigma^2}}$$

Choosing

$$A_0 = 2.26$$

$$p = 4$$

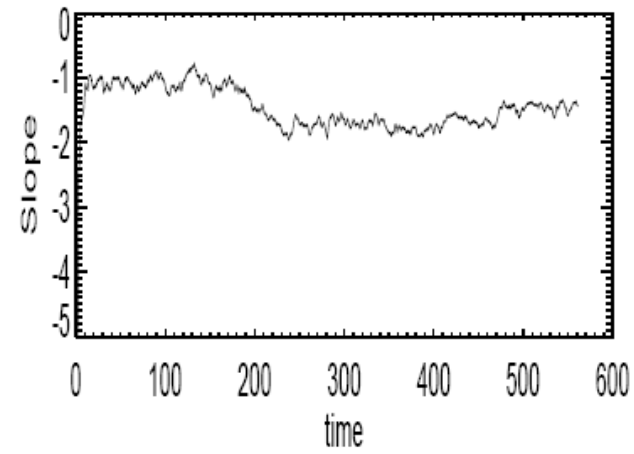
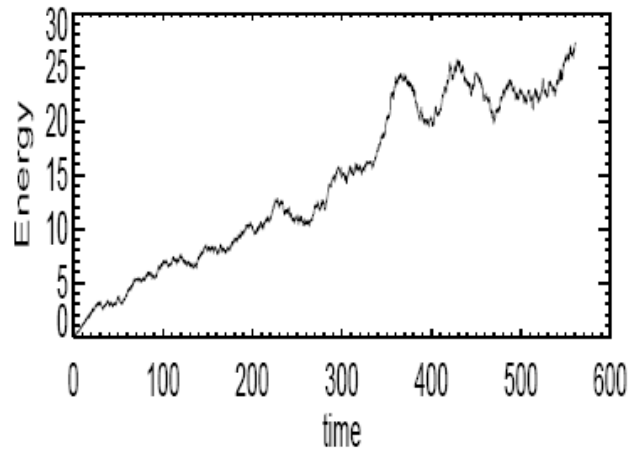
$$\sigma = 0.25$$

$$\beta = 2$$

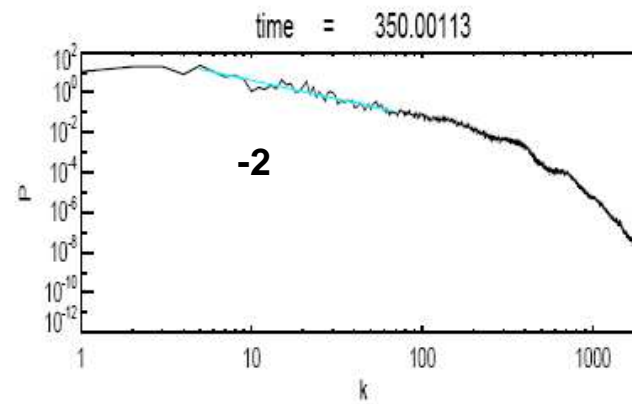
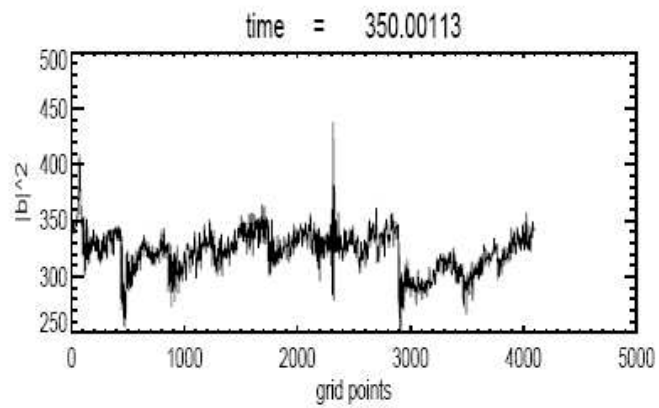
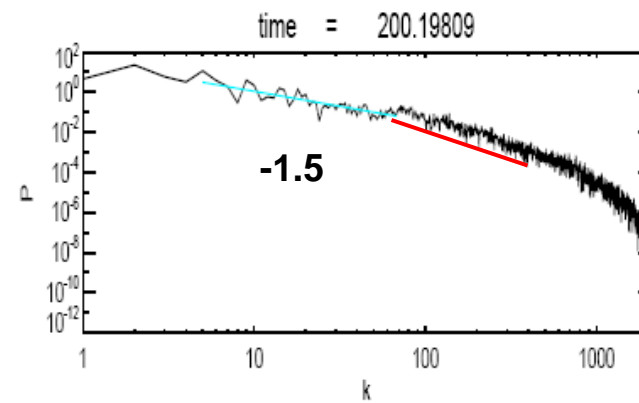
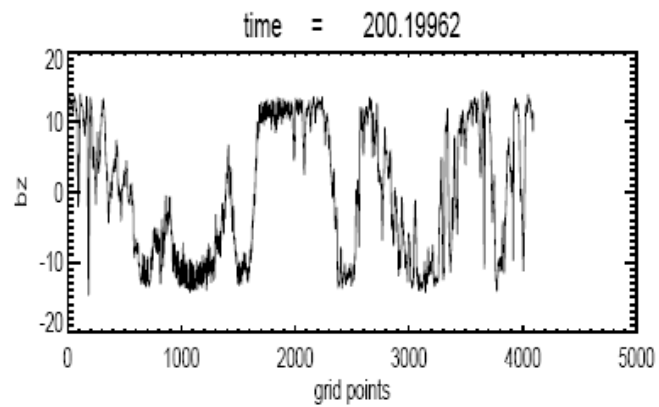
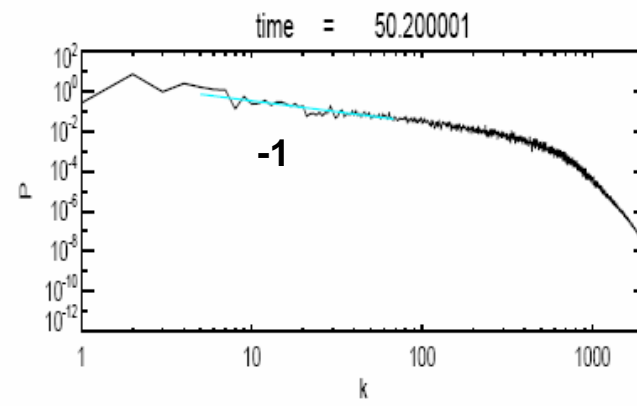
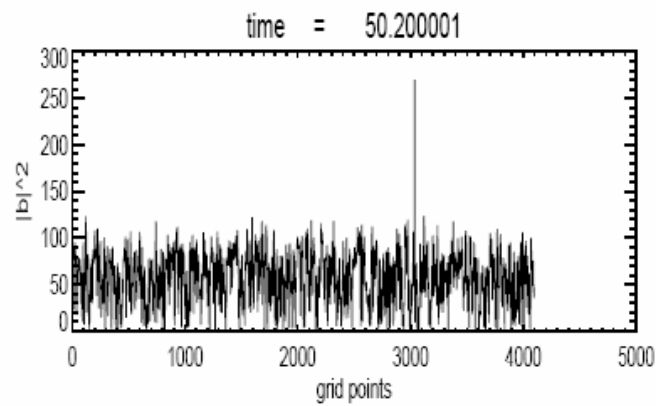
The forcing peaks at $k=4$

Domain size 16π

Simulations with constant Forcing



No extra dissipation is needed



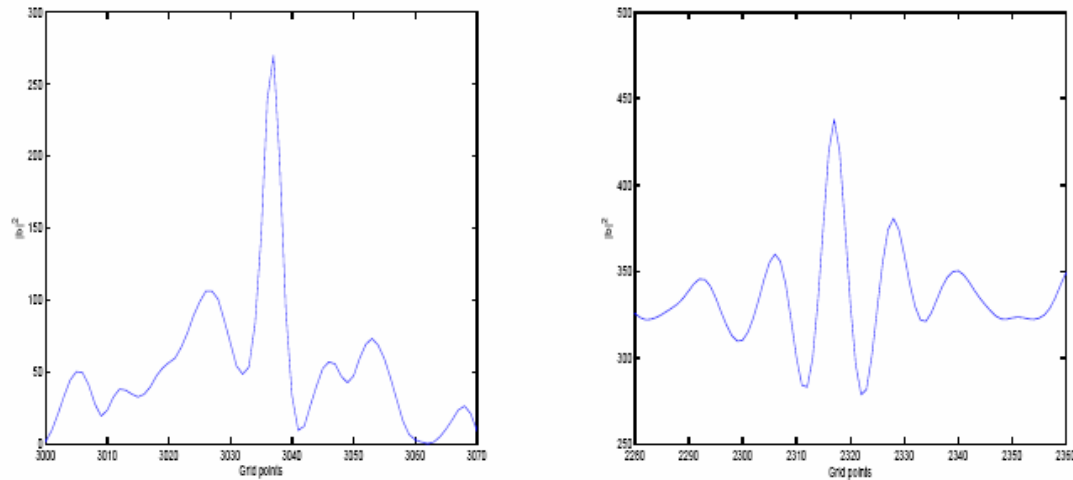
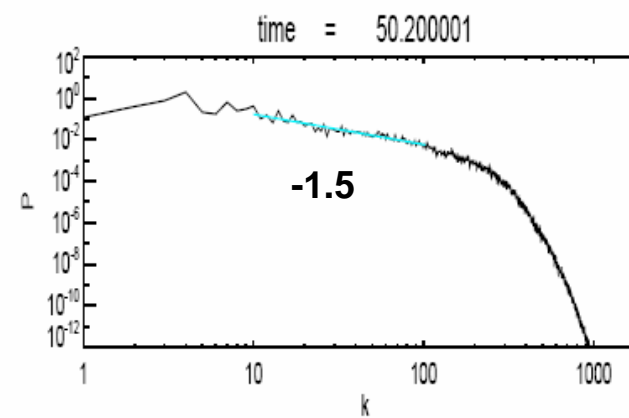
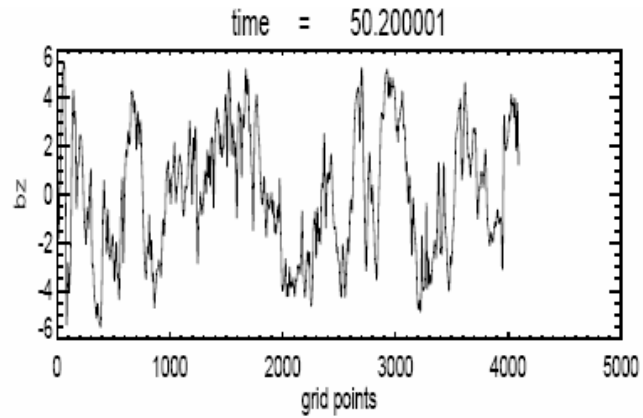
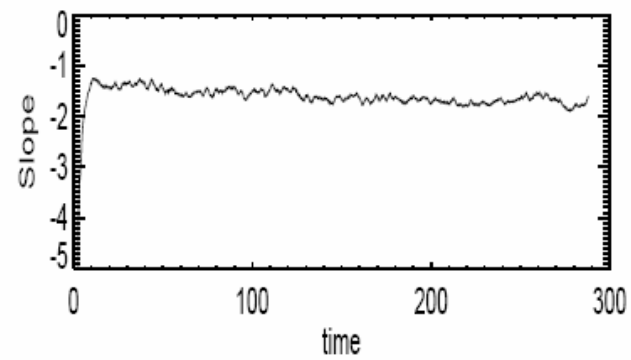
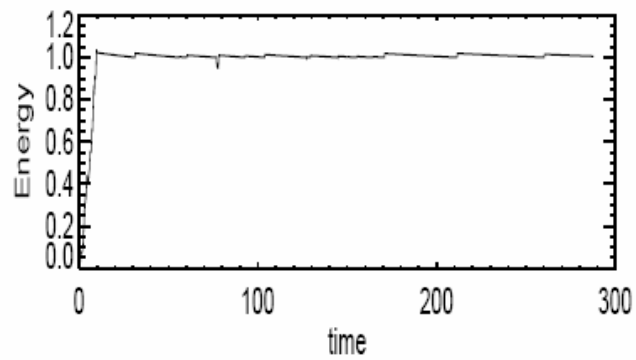


Figure 6: Bright soliton at $t = 50$ and wave-packet like soliton at $t = 350$

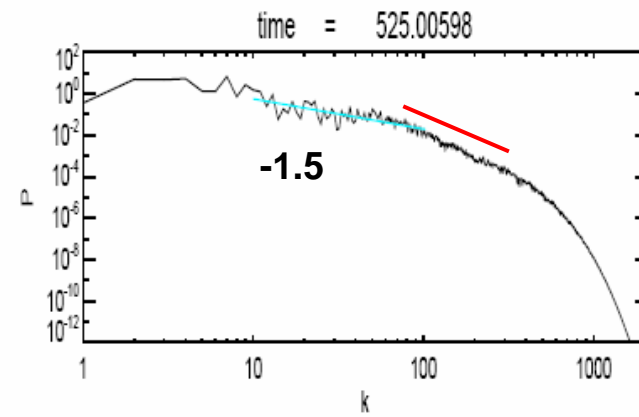
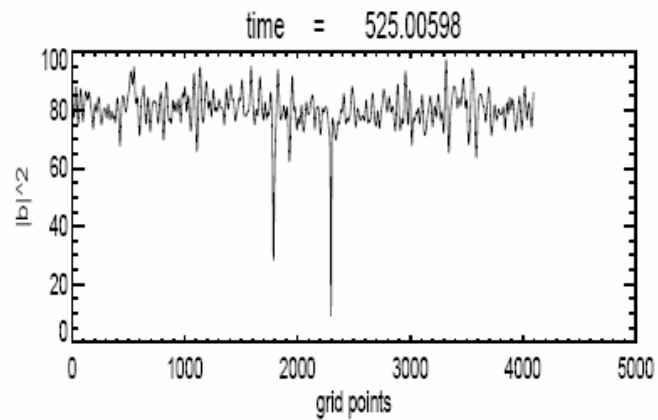
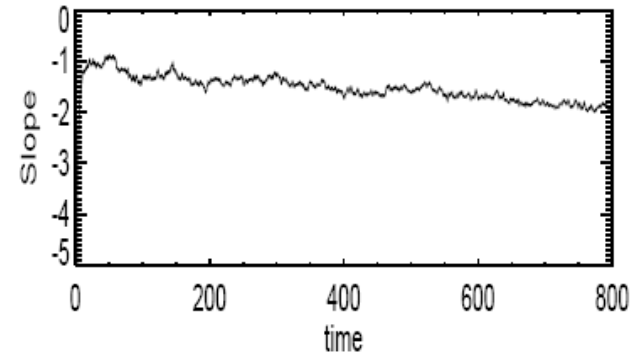
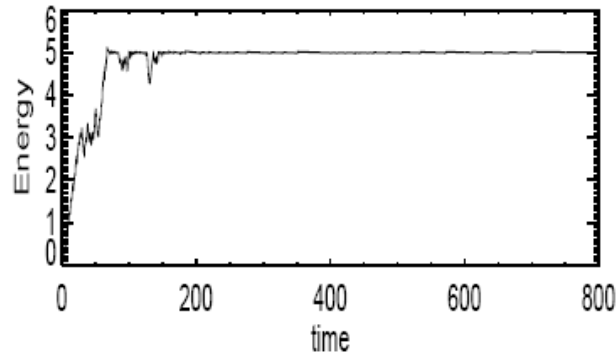
With given parameter solitons of amplitude 1 have width 1.
 The observed high amplitude solitons thus
 obey the DNLS soliton scaling : amplitude $\sim 1/\text{width}$

Situations where the energy is fixed at $E=1$:

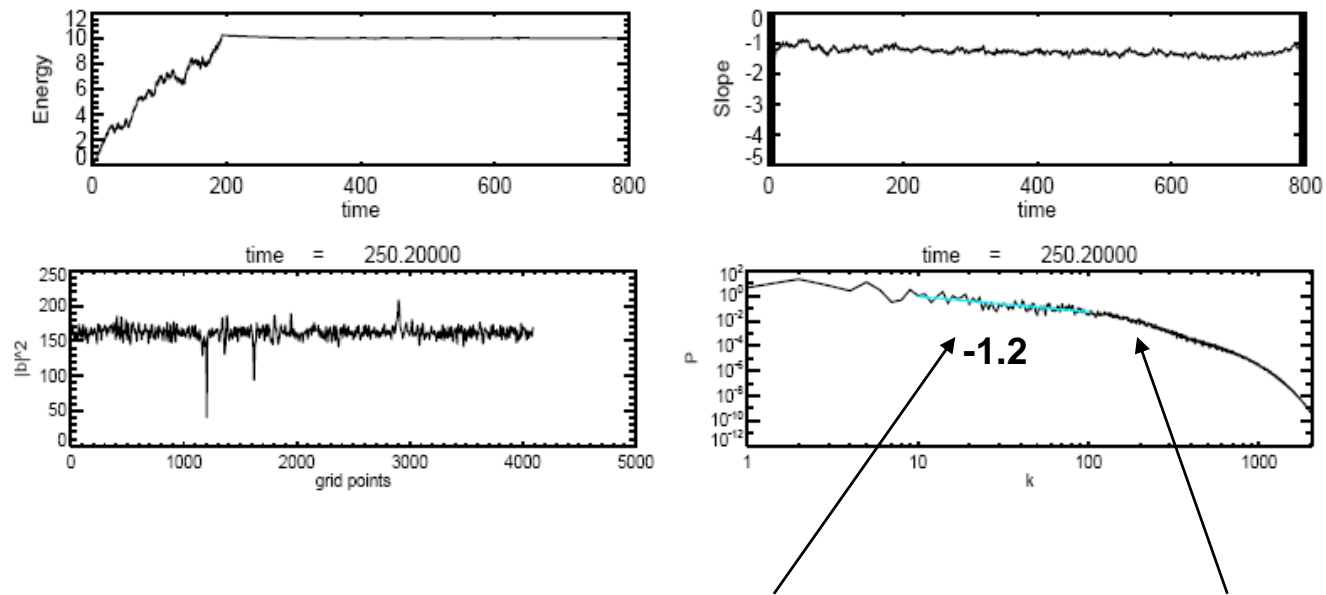


Stirring is minimal: phase coherence can form, leading to the strong turbulence regime

Situations where the energy is fixed at $E=5$:



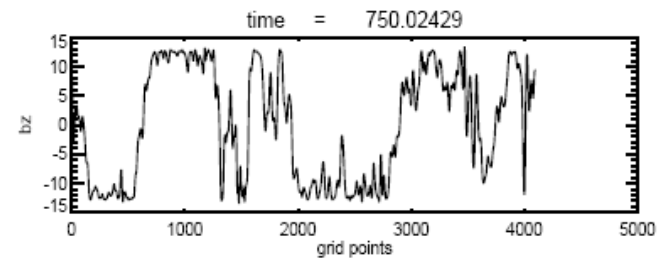
Situations where the energy is fixed at E=10:



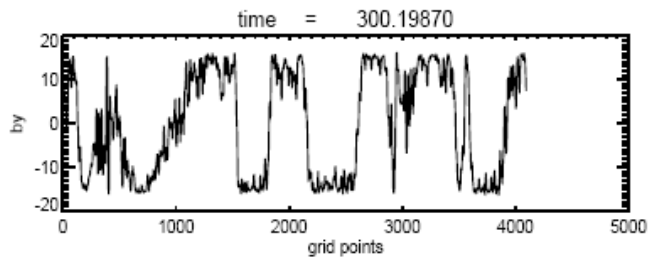
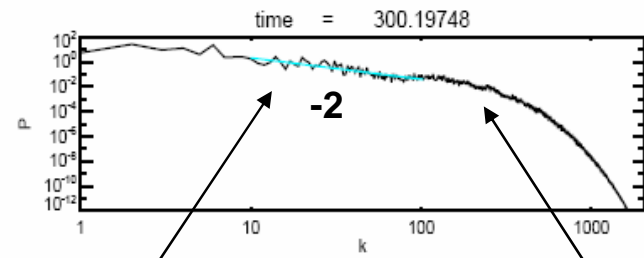
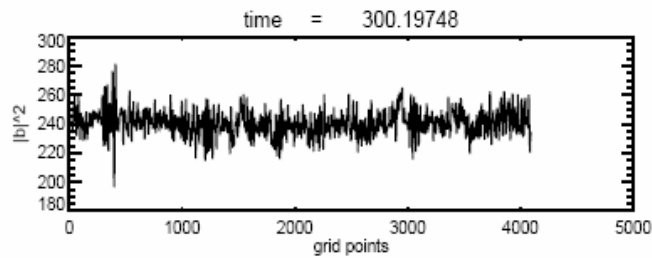
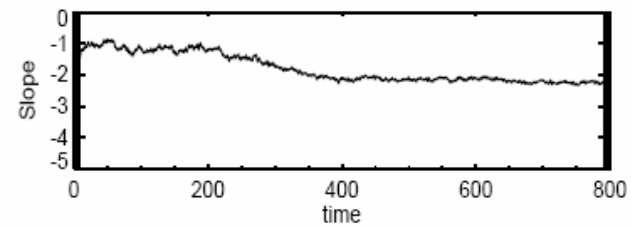
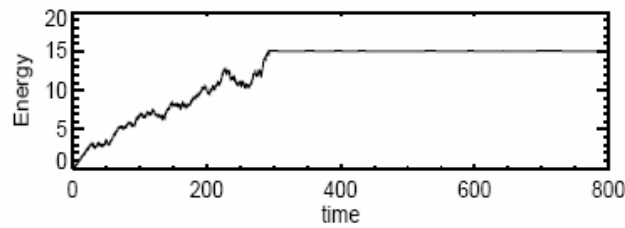
Signature of turbulence

Signature of peak-like structures

Stirring strong enough to allow for wave turbulence with a few solitonic structures.
Shocks are strongly distorted.



Situations where the energy is fixed at E=15:



Signature of shocks: more visible on individual components.

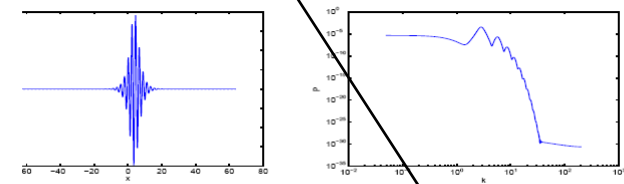
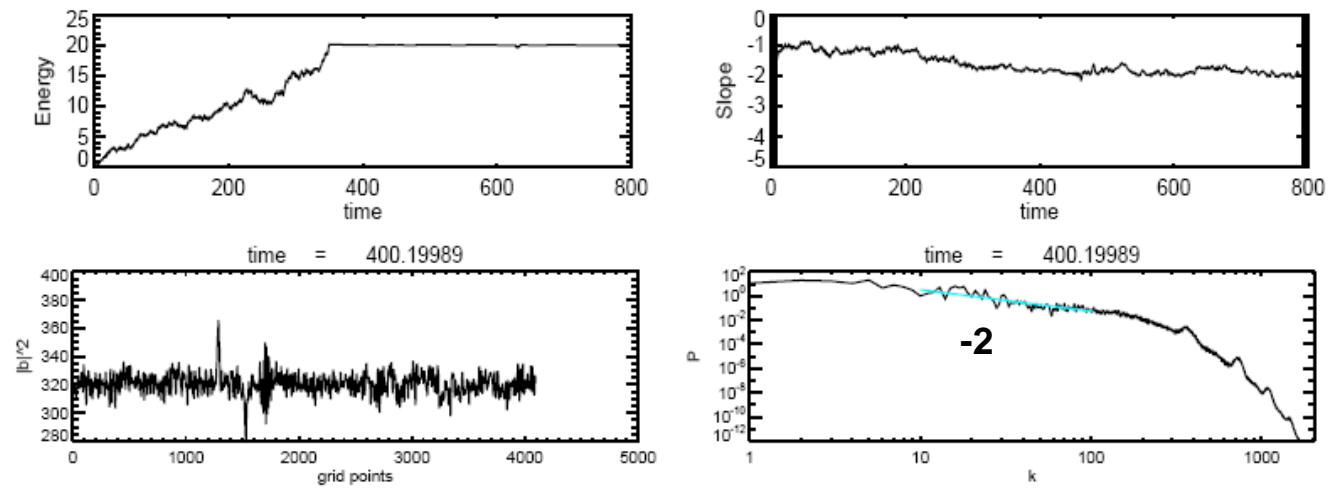


Figure 15: $|b|^2$ and power spectrum of the analytical wave-packet soliton

Signature of wave packets-like structures

Situations where the energy is fixed at $E=20$:



Signature of both peaks and wave packets.

Phenomenology

K41 for hydrodynamic turbulence

$$\epsilon = \frac{kE_k}{\tau_k} \quad \tau_k = \tau_{NL} = \frac{1}{\sqrt{k^3 E_k}} \quad E_k \propto k^{-5/3}$$

Decay time of triple correlations proportional to the turnover time.

MHD (Kraichnan)

$$kE_k = |b_k|^2 = |v_k|^2$$

$$\epsilon = \frac{kE_k}{\tau_{tr}} \quad \tau_{tr}\tau_w = \tau_{NL}^2$$

Decay time of triple correlations proportional to the Alfvén time.

non dispersive MHD :

$$\tau_w = \frac{1}{v_A k}$$

$$\tau_{NL} = \frac{1}{\sqrt{k^3 E_k}} \quad \tau_{tr} = \frac{v_A k}{k^3 E_k} \quad \epsilon = \frac{1}{v_A} k^3 E_k^2 \quad E_k \propto k^{-3/2}$$

Does not take into account anisotropy, coherent structures, intermittency

DNLS

Nondispersive scales:

$$\tau_{tr} = \tau_{NL} \equiv \frac{1}{k|b_k|^2} = \frac{1}{k^2 E_k} \quad \epsilon = k^3 E_k^2 \quad E_k \propto k^{-3/2}$$

When nonlinearity dominates over dispersion: strongly turbulent

Dispersive scales:

$$\tau_w = k^{-2} \quad \tau_{NL} \equiv \frac{1}{k|b_k|^2} = \frac{1}{k^2 E_k} \quad \tau_{tr} = \frac{\tau_{NL}^2}{\tau_w} = \frac{1}{k^2 E_k^2}$$

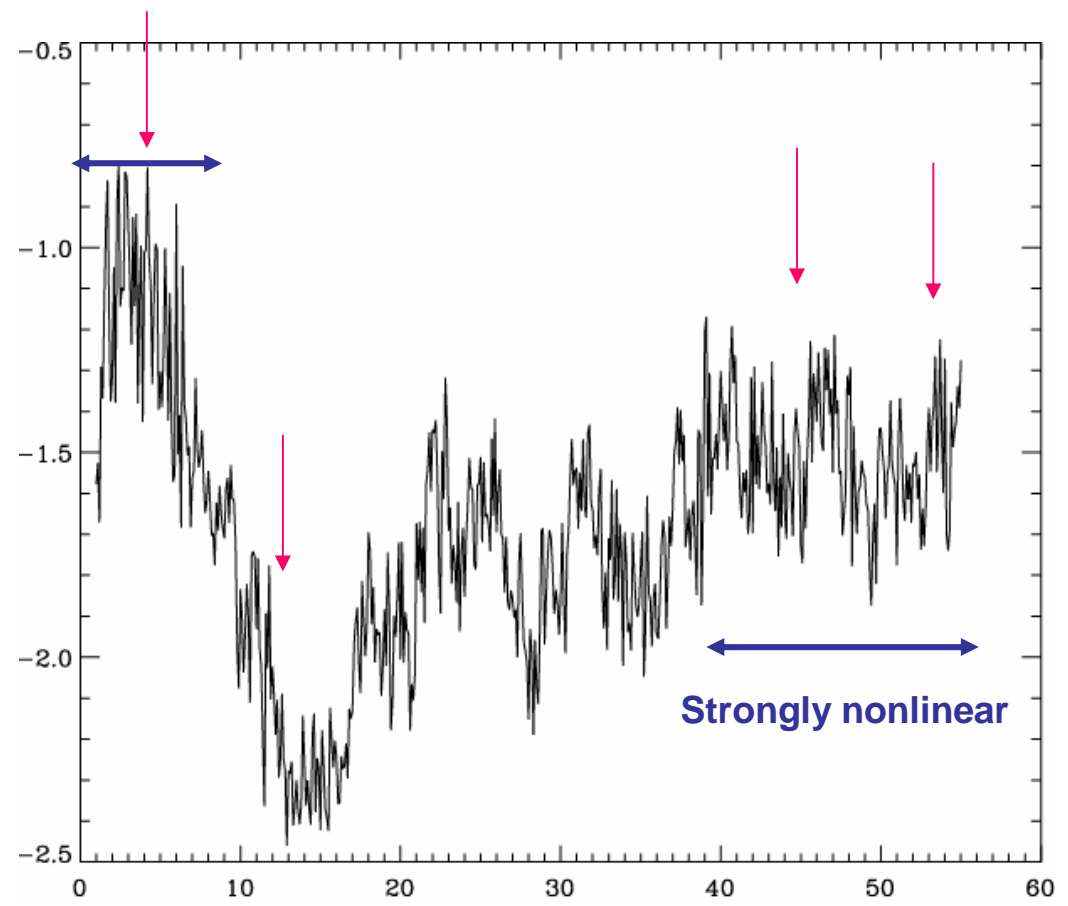
$$\epsilon_N = E_k k^2 E_k^2 = k^3 E_k^3 \quad E_k \propto k^{-1}$$

When nonlinear transfer is slowed down by wave dispersion: not very strong turbulence

In the presence of strong shocks a k^{-2} spectrum is expected

Instantaneous slope vs. time:
Non-stationarity

Nonlinearity affected
by dispersive waves



Development of shocks



Energy builds up

What happens with a more refined model including all types of waves (except Langmuir)?
At first let us examine the 1D case within the context of Landau fluids.

Landau fluids

For the sake of simplicity, neglect electron inertia.

Ion dynamics: derived by computing velocity moments from Vlasov Maxwell equations.

$$\begin{aligned} \partial_t \rho_p + \nabla \cdot (\rho_p u_p) &= 0 & \rho_r &= m_r n_r \\ \partial_t u_p + u_p \cdot \nabla u_p + \frac{1}{\rho_p} \nabla \cdot \mathbf{p}_p - \frac{e}{m_p} (E + \frac{1}{c} u_p \times B) &= 0 & \text{quasi-neutrality } (n_e = n_p) \\ E &= -\frac{1}{c} \left(u_p - \frac{j}{ne} \right) \times B - \frac{1}{ne} \nabla \cdot \mathbf{p}_e, & j &= \frac{c}{4\pi} \nabla \times B \\ \partial_t B &= -c \nabla \times E \end{aligned}$$

$$\mathbf{p}_p = p_{\perp p} \mathbf{n} + p_{\parallel p} \boldsymbol{\tau} + \mathbf{\Pi}, \text{ with } \mathbf{n} = \mathbf{I} - \hat{b} \otimes \hat{b} \text{ and } \boldsymbol{\tau} = \hat{b} \otimes \hat{b}, \text{ where } \hat{b} = \mathbf{B} / |\mathbf{B}|.$$

Electron pressure tensor is taken gyrotropic (scales \gg electron Larmor radius): characterized by the parallel and transverse pressures $p_{\parallel e}$ and $p_{\perp e}$.

For each particle species,

Perpendicular and parallel pressures

$$\begin{aligned} \partial_t p_{\perp} + \nabla \cdot (u p_{\perp}) + p_{\perp} \nabla \cdot u - p_{\perp} \hat{b} \cdot \nabla u \cdot \hat{b} + \frac{1}{2} [\text{tr} \nabla \cdot \mathbf{q} - \hat{b} \cdot (\nabla \cdot \mathbf{q}) \cdot \hat{b}] &= 0 \\ \partial_t p_{\parallel} + \nabla \cdot (u p_{\parallel}) + 2p_{\parallel} \hat{b} \cdot \nabla u \cdot \hat{b} + \hat{b} \cdot (\nabla \cdot \mathbf{q}) \cdot \hat{b} &= 0 \end{aligned}$$

heat flux tensor
↙

Nongyrotropic components (gyroviscous tensor) of the pressure tensor will be evaluated separately by fitting with the linear kinetic theory.

Heat fluxes

$$\mathbf{n} = \mathbf{I} - \hat{\mathbf{b}} \otimes \hat{\mathbf{b}} \text{ and } \boldsymbol{\tau} = \hat{\mathbf{b}} \otimes \hat{\mathbf{b}}, \text{ where } \hat{\mathbf{b}} = \mathbf{B}/|\mathbf{B}|$$

Proton heat flux tensor: $\mathbf{q} = \mathbf{S} + \boldsymbol{\sigma}$ with $\sigma_{ijk}n_{jk} = 0$ and $\sigma_{ijk}\tau_{jk} = 0$.

↑
Nongyrotropic tensor that contributes
at the nonlinear level only

Fluxes of parallel and transverse heat: $S_i^{\parallel} = q_{ijk}\tau_{jk}$ and $2S_i^{\perp} = q_{ijk}n_{jk}$.

Parallel heat fluxes of perpendicular and parallel heat $q_{\perp} = S^{\perp} \cdot \hat{\mathbf{b}}$ and $q_{\parallel} = S^{\parallel} \cdot \hat{\mathbf{b}}$ are the only contribution to the gyrotropic heat flux tensor.

Write $S^{\perp} = q_{\perp}\hat{\mathbf{b}} + S_{\perp}^{\perp}$ and $S^{\parallel} = q_{\parallel}\hat{\mathbf{b}} + S_{\perp}^{\parallel}$ where the perpendicular heat flux of perpendicular and parallel heat S_{\perp}^{\perp} and S_{\perp}^{\parallel} are computed in a linearized approximation.

The gyrotropic heat flux components q_{\perp} and q_{\parallel} obey dynamical equations.

Equations for the parallel and perpendicular (gyrotropic) heat fluxes

$$\left\{ \begin{array}{l} \partial_t q_{\parallel} + \nabla \cdot (q_{\parallel} u) + 3q_{\parallel} \hat{b} \cdot \nabla u \cdot \hat{b} + 3p_{\parallel} (\hat{b} \cdot \nabla) \left(\frac{p_{\parallel}}{\rho} \right) + \nabla \cdot (\tilde{r}_{\parallel\parallel} \hat{b}) - 3\tilde{r}_{\parallel\perp} \nabla \cdot \hat{b} + \partial_z R_{\parallel}^{NG} = 0 \\ \partial_t q_{\perp} + \nabla \cdot (u q_{\perp}) + q_{\perp} \nabla \cdot u + p_{\parallel} (\hat{b} \cdot \nabla) \left(\frac{p_{\perp}}{\rho} \right) + \frac{p_{\perp}}{\rho} (\partial_x \Pi_{xz} + \partial_y \Pi_{yz}) \\ + \nabla \cdot (\tilde{r}_{\parallel\perp} \hat{b}) + \left((p_{\parallel} - p_{\perp}) \frac{p_{\perp}}{\rho} - \tilde{r}_{\perp\perp} + \tilde{r}_{\parallel\perp} \right) (\nabla \cdot \hat{b}) + \partial_z R_{\perp}^{NG} = 0 \end{array} \right.$$

Involve the 4 th rank gyrotropic cumulants $\tilde{r}_{\parallel\parallel}, \tilde{r}_{\parallel\perp}, \tilde{r}_{\perp\perp}$
expressed in terms of the 4 th rank gyrotropic moments by

$$\tilde{r}_{\parallel\parallel} = r_{\parallel\parallel} - 3 \frac{p_{\parallel}^2}{\rho},$$

$$\tilde{r}_{\parallel\perp} = r_{\parallel\perp} - \frac{p_{\perp} p_{\parallel}}{\rho},$$

$$\tilde{r}_{\perp\perp} = r_{\perp\perp} - 2 \frac{p_{\perp}^2}{\rho}.$$

R_{\parallel}^{NG} and R_{\perp}^{NG} stand for the nongyrotropic contributions of the fourth rank cumulants.

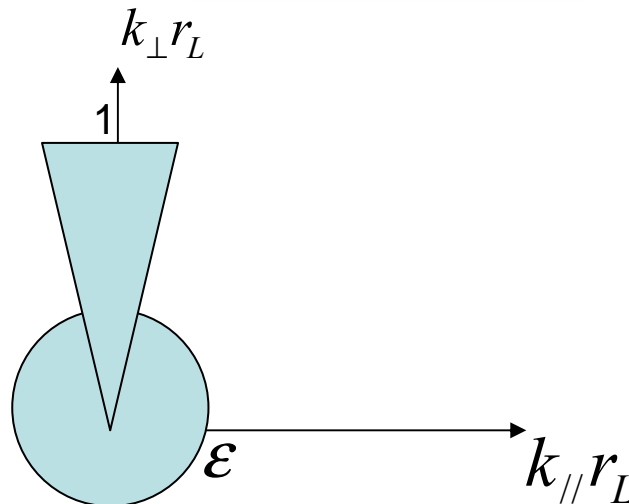
2 main problems:

- (1) Closure relations are needed to express the 4th order cumulants $\tilde{r}_{\parallel\parallel\parallel}, \tilde{r}_{\parallel\perp\perp}, \tilde{r}_{\perp\perp\perp}$ (closure at lowest order also possible, although usually less accurate)
- (2) FLR corrections (non-gyrotropic) to the various moments are to be evaluated

The starting point for addressing these points is the **linear kinetic theory in the low-frequency limit**. $\omega/\Omega \sim \epsilon \ll 1$ (Ω : ion gyrofrequency)

For a unified description of fluid and kinetic scales, FLR-Landau fluids retain contributions of:

- quasi-transverse fluctuations $(k_{\parallel}/k_{\perp} \sim \epsilon)$ with $k_{\perp}r_L \sim 1$
- hydrodynamic scales with $k_{\parallel}r_L \sim k_{\perp}r_L \sim \epsilon$. r_L : ion Larmor radius



CLOSURE RELATIONS are based on linear kinetic theory (near bi-Maxwellian equilibrium) in the low-frequency limit.

For example, for each species, (assuming the ambient magnetic field along the z direction),

$$\tilde{r}_{\parallel\perp} = \frac{p_{\perp}^{(0)2}}{\rho^{(0)}} \left[1 - R(\zeta) + 2\zeta^2 R(\zeta) \right] \left[[2b\Gamma_0(b) - \Gamma_0(b) - 2b\Gamma_1(b)] \frac{b_z}{B_0} + b[\Gamma_0(b) - \Gamma_1(b)] \frac{e\Psi}{T_{\perp}^{(0)}} \right]$$

$$\Gamma_n(b) = e^{-b} I_n(b), \quad b = (k_{\perp}^2 T_{\perp}^{(0)}) / (\Omega^2 m), \quad I_n(b) \text{ modified Bessel function, } E_z = -\partial_z \Psi$$

R is the plasma response function, $\zeta = \frac{\omega}{|k_{\parallel}| v_{th}}$. (For electrons, $b \approx 0$, $\Gamma_0 \approx 1$, $\Gamma_1 \approx 0$)

It turns out that $\tilde{r}_{\parallel\perp}$ can be expressed in terms of perpendicular gyrotropic heat flux q_{\perp} and of the parallel current j_z . One has

$$\tilde{r}_{\parallel\perp} = \sqrt{\frac{2T_{\parallel}^{(0)}}{m} \frac{1 - R(\zeta) + 2\zeta^2 R(\zeta)}{2\zeta R(\zeta)}} \left[q_{\perp} + [\Gamma_0(b) - \Gamma_1(b)] \frac{p_{\perp}^{(0)} p_{\parallel}^{(0)}}{\rho^{(0)} v_A^2} \left(\frac{T_{\perp}^{(0)}}{T_{\parallel}^{(0)}} - 1 \right) \frac{j_z}{en^{(0)}} \right]$$

The **approximation** consists in replacing the plasma response function R by the three pole Padé approximant $R_3(\zeta) = \frac{2 - i\sqrt{\pi}\zeta}{2 - 3i\sqrt{\pi}\zeta - 4\zeta^2 + 2i\sqrt{\pi}\zeta^3}$.

This leads to the approximation $\frac{1 - R(\zeta) + 2\zeta^2 R(\zeta)}{2\zeta R(\zeta)} \approx \frac{i\sqrt{\pi}}{-2 + i\sqrt{\pi}\zeta}$.

(A lower order Padé approximant would overestimate the Landau damping in the large ζ limit).

One finally gets a closure relation in the form of the evolution equation (for each species)

$$\left[\frac{d}{dt} - \frac{2}{\sqrt{\pi}} \sqrt{\frac{2T_{\parallel}^{(0)}}{m}} \mathcal{H}_z \partial_z \right] \tilde{r}_{\parallel\perp} + \frac{2T_{\parallel}^{(0)}}{m} \partial_z [q_{\perp} + [\Gamma_0(b) - \Gamma_1(b)] \frac{p_{\perp}^{(0)} p_{\parallel}^{(0)}}{\rho^{(0)} v_A^2} \left(\frac{T_{\perp}^{(0)}}{T_{\parallel}^{(0)}} - 1 \right) \frac{j_z}{en^{(0)}}] = 0,$$

In Fourier space, Hilbert transform \mathcal{H}_z reduces to the multiplication by $i \operatorname{sgn} k_z$.

Improvement: Retain the evolution of the equilibrium state by replacing the (initial) equilibrium pressures and temperatures by the instantaneous fields averaged on space.

In the large-scale limit, $\Gamma_0(0) = 1$ and $\Gamma_1(0) = 0$.

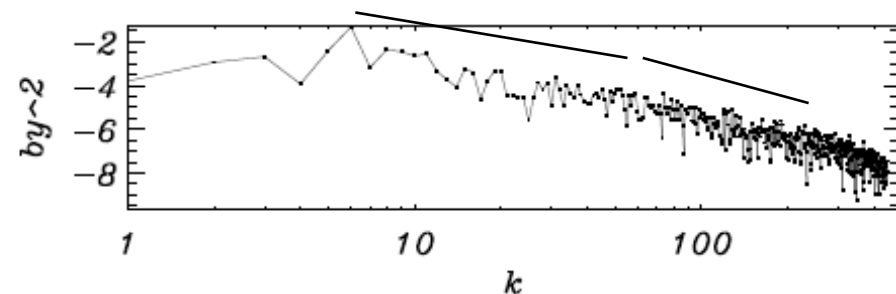
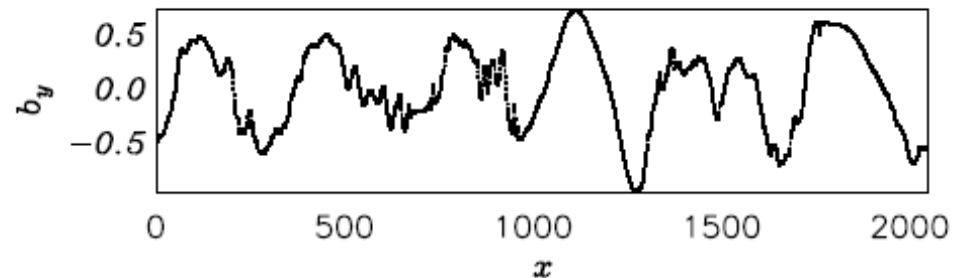
A 1D SIMULATION

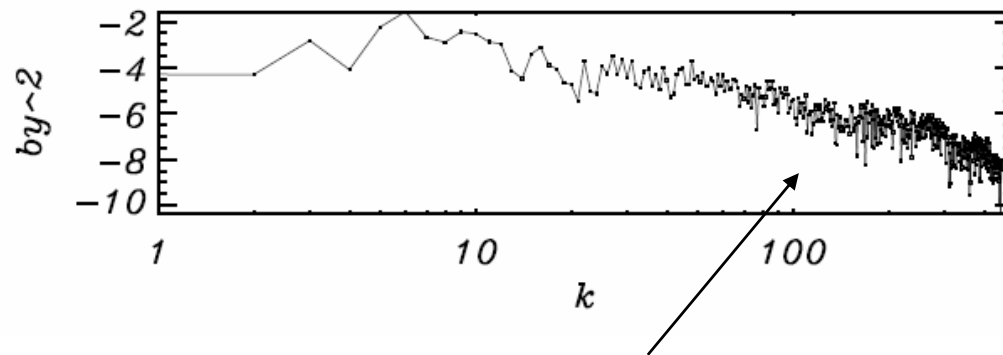
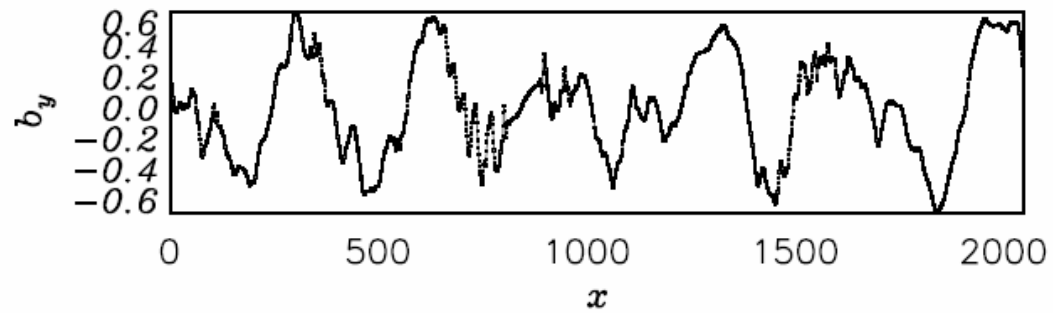
with:

- A small amount of collisions to let parallel and perpendicular pressures tend to the same mean values and thus avoid instabilities.
- Random forcing of the three velocity components between $k=2$ and 10 , peaking at $k=5$, only on when the total energy falls below prescribed value.
- Angle of propagation: 84°
- $\beta=1$, $T_e/T_i=5$
- Size of the domain: $300 \times 2\pi$
- No extra dissipation

A **break** in the spectrum starts to develop at a nonlinear **dispersive scale**

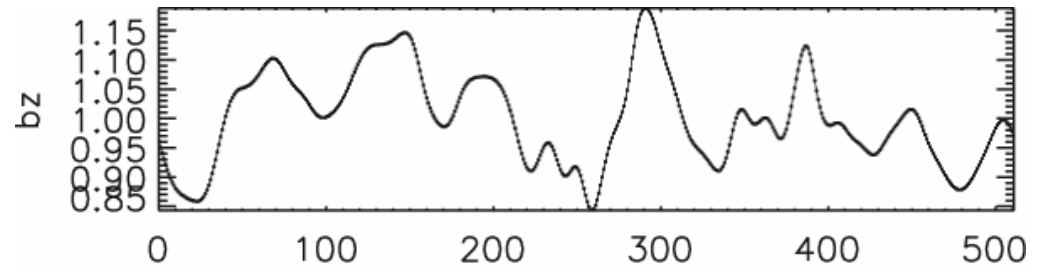
In spite of superimposed turbulence, **large-scale structures** form.



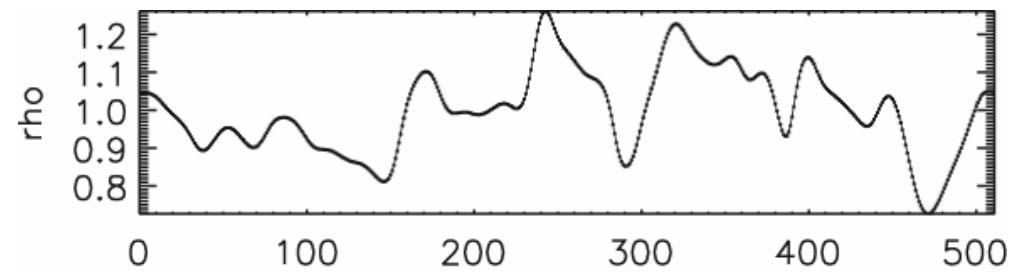
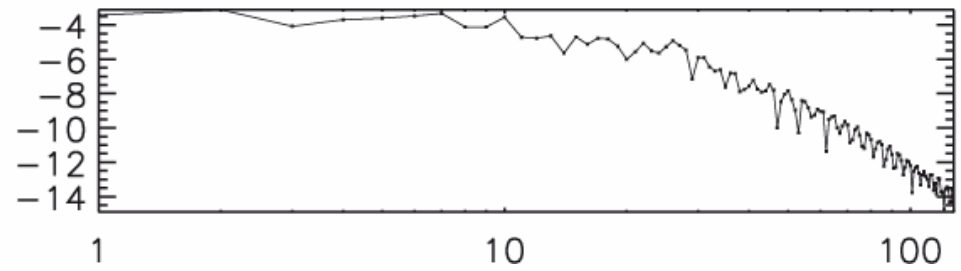


Signature of wave packets

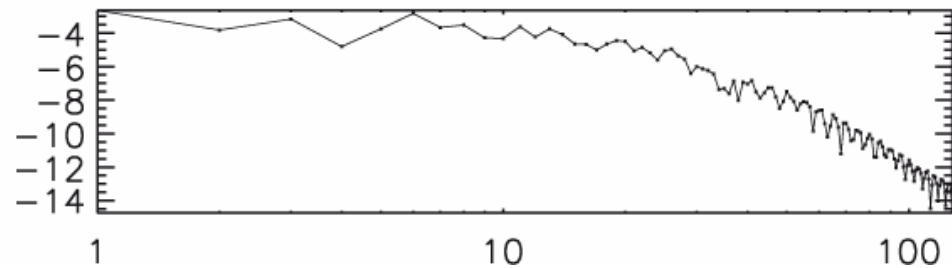
(another simulation
at lower resolution)



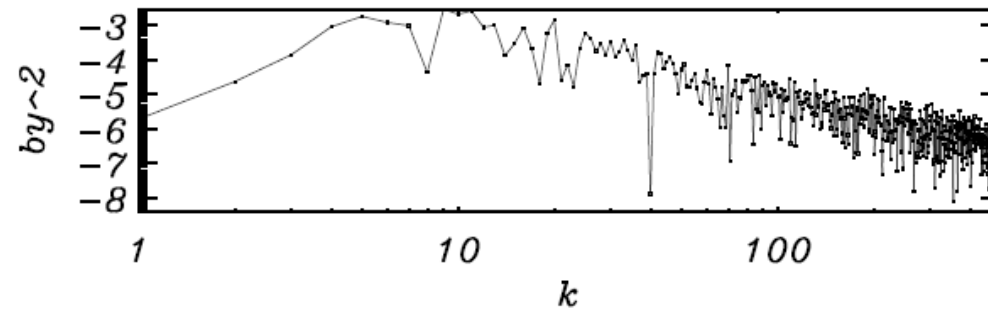
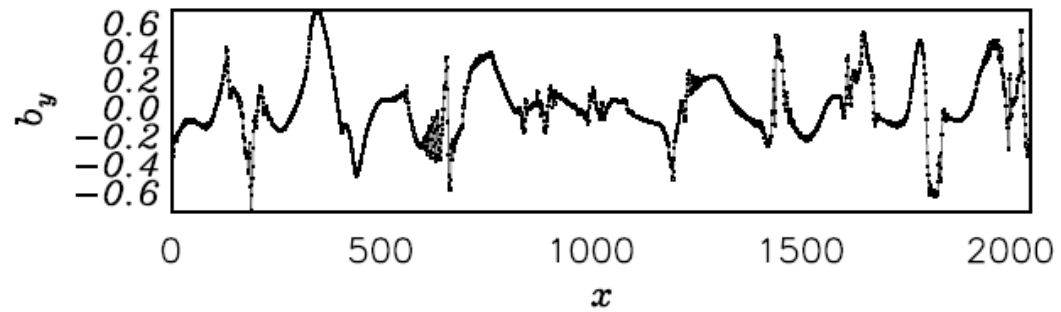
Longitudinal field



Density



Parallel propagation



Domain size: 600π

Hall-MHD equations with a polytropic equation of state

$$\partial_t \rho + \nabla \cdot (\rho \mathbf{u}) = 0$$

$$\rho(\partial_t \mathbf{u} + \mathbf{u} \cdot \nabla \mathbf{u}) = -\frac{\beta}{\gamma} \nabla \rho^\gamma + (\nabla \times \mathbf{b}) \times \mathbf{b}$$

$$\partial_t \mathbf{b} - \nabla \times (\mathbf{u} \times \mathbf{b}) = -\frac{1}{R_i} \nabla \times \left(\frac{1}{\rho} (\nabla \times \mathbf{b}) \times \mathbf{b} \right)$$

$$\nabla \cdot \mathbf{b} = 0$$

velocity unit: Alfvén speed

length unit : $R_i \times$ ion inertial length

time unit: $R_i \times$ ion gyroperiod

density unit: mean density

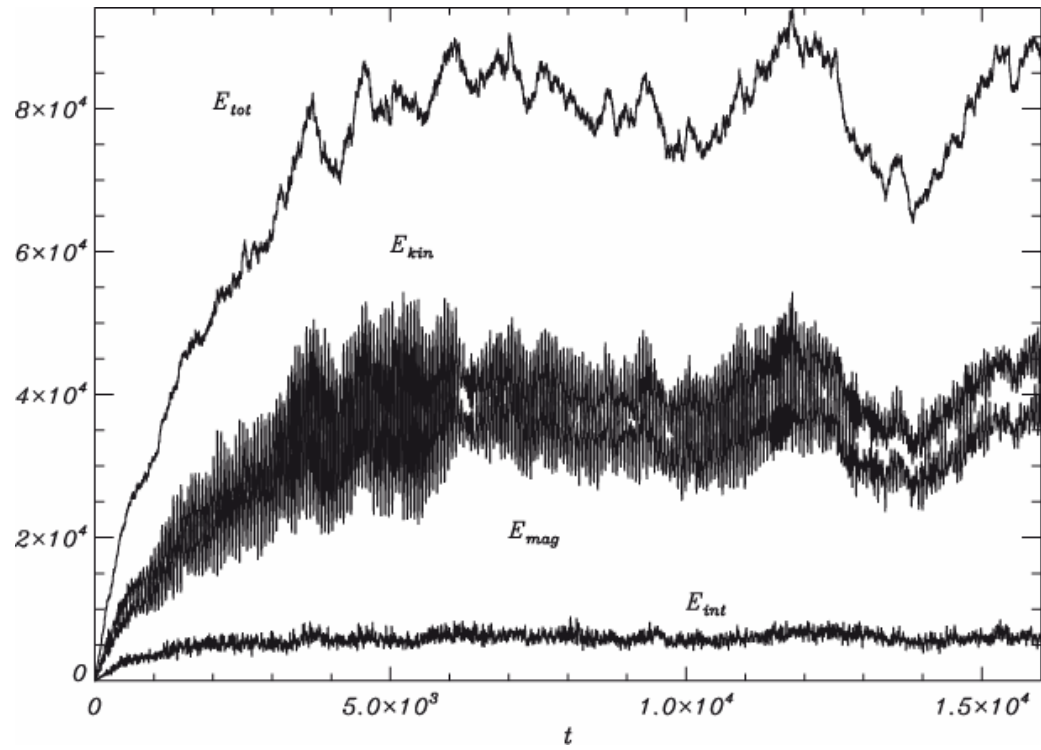
magnetic field unit: ambient field

2D simulations with uniform field in the z-direction

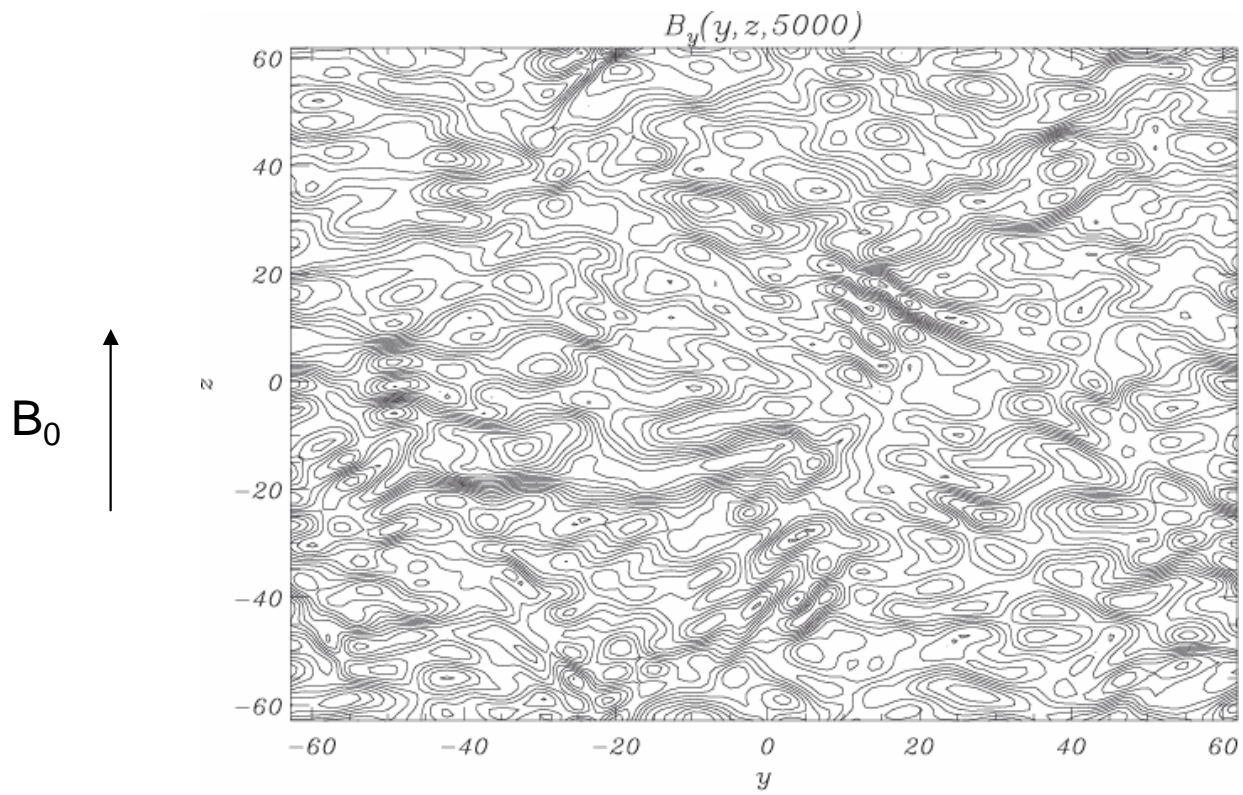
Forcing of the transverse velocity field components at $k=2$

Parameters: $\beta=1$, $\gamma=2$, $R_i=1$, size of domain= $20 \times 2 \times \pi$

A filter is used to dissipate.



Evolution of the energy as a function of time

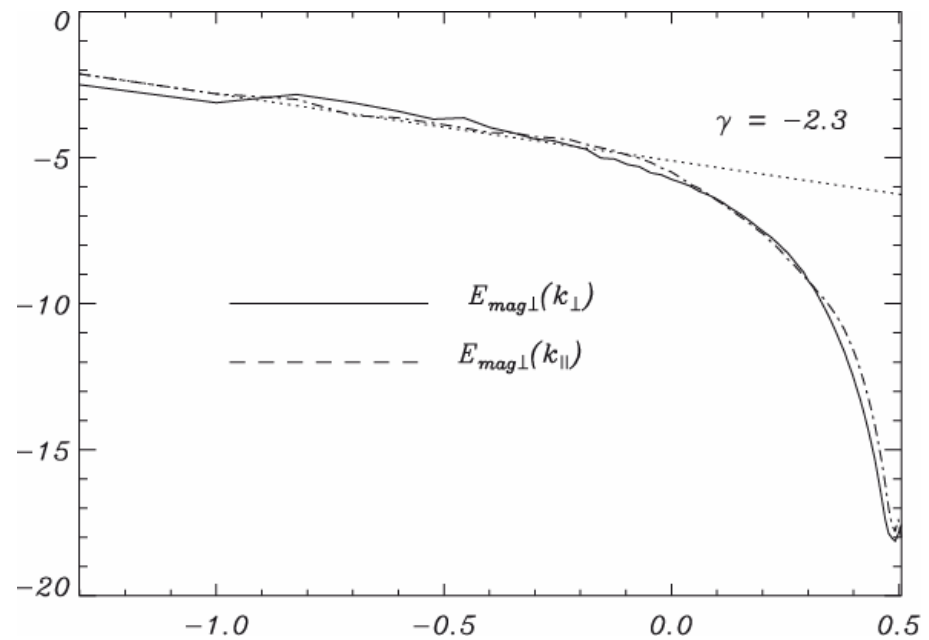
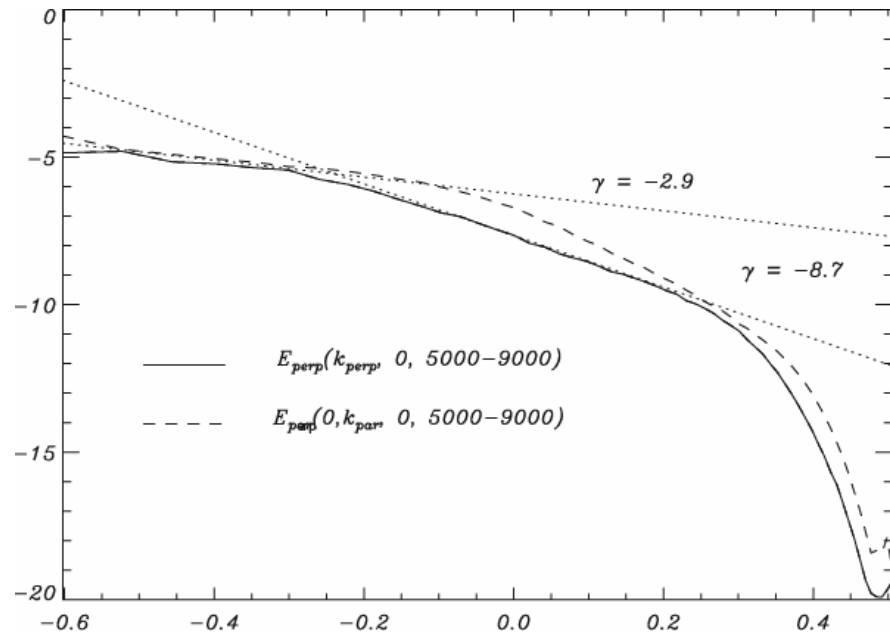


Typical contour plot of B_y field

Spectra of perpendicular magnetic energy as a function of k_{\perp} (for $k_{\parallel}=0$): solid and as a function of k_{\parallel} (for $k_{\perp}=0$): dashed

A break is observed with a steeper slope at small scales. In the parallel direction, the spectrum drops off more quickly but the large-scale range extends to smaller scales.

Spectra of perpendicular magnetic energy as a function of k_{\perp} (summed over all k_{\parallel}): solid and as a function of k_{\parallel} (summed over all k_{\perp}): dashed



Conclusions

Dispersion does not prevent the formation of small scales and the development of a turbulent cascade. Coherent structures nevertheless form.

A break in the spectrum at the dispersive scale is directly observed in DNLS, Landau fluid and Hall-MHD simulations, although the mechanisms are very different.

Further work is needed to identify whether it corresponds to the ion gyro-radius or the ion inertial length.

Further work is also necessary to explore the dynamics of KAWs, in particular for smaller values of T_e/T_i and/or at smaller scales. Purely kinetic numerical study is probably needed in this case.

Three-dimensional simulations are underway.